

NSWCDD/TR-92/218

AD-A264 482



**THE MEASUREMENT OF ELECTRICAL
CONDUCTIVITY IN DETONATING
CONDENSED EXPLOSIVES**

BY DOUGLAS G. TASKER, RICHARD J. LEE, and PAUL K. GUSTAVSON

WEAPONS RESEARCH AND TECHNOLOGY DEPARTMENT

MARCH 1993

DTIC
ELECTE
MAY 19 1993
S & D

Approved for public release; distribution is unlimited.



NAVAL SURFACE WARFARE CENTER

Dahlgren, Virginia 22448-5000 • Silver Spring, Maryland 20903-5000

93 5 18 09 1

93-11140



NSWCDD/TR-92/218

THE MEASUREMENT OF ELECTRICAL CONDUCTIVITY IN DETONATING CONDENSED EXPLOSIVES

BY DOUGLAS G. TASKER , RICHARD J. LEE, and PAUL K. GUSTAVSON

WEAPONS RESEARCH AND TECHNOLOGY DEPARTMENT

MARCH 1993

Approved for public release; distribution is unlimited

NAVAL SURFACE WARFARE CENTER

Dahlgren, Virginia 22448-5000 • Silver Spring, Maryland 20903-5000

FOREWORD

The electrical conductivity of a number of detonating explosives are reported. The results show the conductivity to be sensitive to detonation wave instabilities. The conductivity profile observed in the aluminized explosive PBXN-111 (formerly PBXW-115) is interesting and unusual. The results are probably due to a combination of wave instabilities and late reaction effects, in either aluminum or ammonium perchlorate, or both. The results demonstrate the power of conductivity measurement as a diagnostic tool; wave instabilities are apparent that could not be determined by other means.

We are indebted to Dr. A. Roberts of the Office of Naval Research for his support under Code 123, Project 02403SB, "Electrically Enhanced Detonation."

The excellent scientific contributions by R. Granholm and P. Gustavson to these studies are acknowledged. Grateful thanks to R. Hay, N. Snowden, B. Snowden, H. Gillum (deceased), C. Sorrels (deceased), R. Baker, and many others for their fine experimental work. Special thanks to Dr. J. Forbes for many helpful discussions and encouragement, especially related to the roles of ammonium perchlorate and aluminum in detonation reaction.

Approved by:

William H. Bohli

WILLIAM H. BOHLI, Acting Head
Energetic Materials Division

Accession For	
NTIS GR&I	<input checked="" type="checkbox"/>
DTIC TAB	<input type="checkbox"/>
Unannounced	<input type="checkbox"/>
Justification	
By	
Distribution/	
Availability Codes	
Dist	Avail and/or Special
A-1	

ABSTRACT

The time-resolved measurement of electrical conductivity provides a unique means of studying detonating explosives. The results of a large number of experiments are reported. Two types of experiments were performed; they measured bulk resistance and time-resolved conductivity. Some interesting effects, due to detonation wave instabilities, were observed when the explosives' dimensions were close to criticality, i.e., close to failure diameter or thickness.

The conductivity profile observed in the aluminized explosive PBXN-111 (formerly PBXW-115) is interesting and unusual. The results are probably due to a combination of wave instabilities and late reaction effects. This demonstrates one of the advantages of using conductivity measurement as a diagnostic tool. Wave instabilities are apparent that could not be determined by other means.

CONTENTS

<u>Chapter</u>		<u>Page</u>
1	INTRODUCTION	1-1
2	ELECTRICAL MEASUREMENT TECHNIQUES	2-1
3	CONDUCTIVITY-DISTANCE DATA OBTAINED FROM BULK RESISTANCE MEASUREMENTS	3-1
4	CONDUCTIVITY OF DETONATING ALUMINIZED EXPLOSIVE	4-1
5	TIME RESOLVED CONDUCTIVITY MEASUREMENTS	5-1
6	DISCUSSION AND CONCLUSIONS	6-1
	REFERENCES	7-1
 <u>Appendix</u>		
A	THE VERIFICATION OF DETONATION IN SHEETS OF PBXN-111	A-1

ILLUSTRATIONS

<u>Figure</u>		<u>Page</u>
2-1	BASIC CONDUCTIVITY MEASUREMENT CIRCUIT	2-2
3-1	COAXIAL RESISTANCE MEASUREMENT	3-3
3-2	VOLTAGE AND CURRENT DATA FOR PBX-9404 IN THE COAXIAL EXPERIMENT	3-5
3-3	VOLTAGE AND CURRENT DATA FOR PBXW-113(I) IN THE COAXIAL EXPERIMENT	3-6
3-4	VOLTAGE VS. CURRENT AND di/dt VS. TIME FOR PBXW-113(I) IN THE COAXIAL EXPERIMENT	3-7
3-5	PLANAR RESISTANCE MEASUREMENT EXPERIMENT	3-9
3-6	VOLTAGE AND CURRENT DATA FOR PBX-9501 IN THE PLANAR EXPERIMENT	3-10
4-1	APPARATUS TO MEASURE CONDUCTIVITY STRUCTURE IN PBXN-111 USING GUARD-ELECTRODES, A. TOP VIEW OF ELECTRODE, B. END VIEW FROM BOOSTER	4-3
4-2	PBXN-111 RESISTANCE MEASUREMENT APPARATUS, EXPLODED VIEW	4-4
4-3	VOLTAGE AND CURRENT MEASUREMENTS IN DETONATING PBXN-111, FIRST EXPERIMENT	4-6
4-4	VOLTAGE AND CURRENT MEASUREMENTS IN DETONATING PBXN-111, SECOND EXPERIMENT	4-7
5-1	TIME RESOLVED CONDUCTIVITY EXPERIMENT SHOWING CONDUCTION ZONE MOVING FROM LEFT TO RIGHT	5-2
5-2	A. CLOSE-UP OF CONDUCTION PATHS AROUND SLIT B. CONDUCTIVITY PROFILE ADJACENT TO SLIT	5-3
5-3	PBX-9501 CONDUCTIVITY STRUCTURES FOR THICKNESSES OF 1 mm AND 2 mm	5-6
A-1	DETONATION VERIFICATION EXPERIMENT	A-2

TABLES

<u>Table</u>		<u>Page</u>
3-1	COAXIAL TUBE DIMENSIONS	3-2
3-2	COAXIAL RESISTANCE MEASUREMENTS	3-4
3-3	PLANAR CONDUCTIVITY σ_{Δ} PRODUCTS	3-11
A-1	TEST CONFIGURATIONS AND RESULTS	A-1

CHAPTER 1

INTRODUCTION

The time resolved measurement of electrical conductivity provides a unique means of studying detonating explosives. These measurements offer new insights into the physics and chemistry of detonation.

Much work has been done in an effort to understand the electrical conduction in detonating explosives that are subjected to high electric fields.¹ The methods that have been developed are used as tools for probing the detonation process; in particular, they can be used to study the effects of detonation wave stability and the roles of carbon and aluminum during the detonation process.

In this report the results of a large number of experiments are reported. The data are summarized for two types of experiment, bulk resistance and time resolved conductivity measurements, and are interpreted in the light of our existing understanding.

DETONATION CONDUCTION MODELS

Various models of conduction have been considered during the course of these studies. The three main candidates for conduction that have been considered are: shock induced conduction in the unreacted explosive due to band gap reduction, shock induced conduction in the reaction products, and conduction in coagulated carbon behind the reaction zone.

The first model, due to Crawford, assumes that conduction occurs in the unreacted explosive in the von-Neumann spike.² The unreacted explosive at atmospheric pressure behaves as an insulator with a relatively large energy gap, E_g , between the valence and conduction bands; for instance, in TNT $E_g \approx 6.3$ eV. Estimates were made of the reduction of the band gap due to pressure which suggest that TNT becomes an "organic metal" when compressed to 50 percent of its initial volume. This work was not pursued because the experimental data demonstrated that the conduction continued throughout the reaction zone and beyond, as the results below show.

The second model was proposed by Griem.³ For relative simplicity, he assumed that the reaction zone could be represented by a mixture of ionized, atomic species of carbon, hydrogen, nitrogen, and oxygen, C, H, N, and O. Here again, it was assumed that the detonation pressure reduced the band gaps of the atomic species to allow ionization to occur at temperatures of 3000 to 5000°K (i.e., less than 0.5 eV). The preliminary results of this work

suggested that H^- ions were primarily responsible for conduction by liberating electrons that are free to move in a conducting plasma. However, later work showed that at near solid densities H^- ions may not exist. The electrons may "hop" from one H atom to the next behaving as "virtual negative ions." This preliminary study did successfully predict conductivities comparable with experimental results.

Hayes has produced convincing evidence that the conduction may be due to carbon in the products of the detonation gases.⁴ He propagated a non-planar detonation wave into a divergent electric field at the end of a coaxial probe. The interpretation of the data was hampered by the divergent geometry but this classic work was probably the first to demonstrate the use of conductivity measurements to probe the structure of the detonation process. Hayes showed that the peak conductivity, which is perhaps equivalent to the spike reported here in Chapter 5, was strongly correlated to the calculated carbon content of the products.

OVERVIEW OF RESULTS

Bulk Resistance Measurements

The dynamic electrical resistances of detonating explosives were obtained from simultaneous measurements of voltage across the explosives, and current flowing in them, as functions of time. The resistances, R , were obtained from the slopes of voltage, V , versus current, I , i.e., using V - I plots. From these resistances the products of the explosives' conductivities and conduction-zone widths were determined. These V - I plots were typically linear and the lines could be extrapolated through the origin. However, small departures from these lines which occurred at the time the detonation wave first entered the electrodes were detected. These departures were determined to be due to the finite time duration for the conduction zone to enter the electrodes.

It was found that the products of the explosives' conductivities and conduction-zone widths were typically independent of geometry. However, results for PBX-9404 and PBX-9501 showed significant differences. These effects were found to be due to detonation wave instabilities that occur when the explosives' dimensions are close to criticality, i.e., close to failure diameter or thickness.

Conductivity in Aluminized Explosive PBXN-111

The conductivity profile observed in PBXN-111 (formerly PBXW-115) is interesting and unusual. At first the results were interpreted as evidence of late reactions in the explosive. However, there are large variations from experiment to experiment which suggest that the structure is strongly affected by detonation wave instabilities. The results are probably due to a combination of wave instabilities and late reaction effects. This demonstrates one of the advantages of conductivity measurement as a diagnostic tool. Wave instabilities are apparent

that could not be determined by dent testing or ionization pin data; these can be observed in fine detail using the present technique.

Conductivity Structure in PBX-9501

The conductivity structure of PBX-9501 reported in Chapter 5 is particularly interesting. It has been estimated from critical diameter measurements that the reaction zone thickness is approximately $100\text{ }\mu\text{m}$;⁵ this is equivalent to a time duration of only 11 ns. Yet the data presented in Chapter 5 of this report showed conduction spikes of at least 100 ns duration followed by $1\text{ }\mu\text{s}$ duration tails. Several researchers have noted that their models of detonation phenomena do not adequately match observed data unless a slow-burn term for the combustion of carbon is included.^{6,7,8} Johnson⁷ has suggested that carbon slowly coagulates into large clusters behind the detonation front in the product gases. This coagulation provides an additional, slow energy release after the main reaction. These findings are consistent with the conductivity measurements by Hayes and of the work reported here, i.e., that conduction is due to the presence of carbon behind the shock front.

CHAPTER 2

ELECTRICAL MEASUREMENT TECHNIQUES

The conductivity measurements have been performed in two main classes of experiments, those that measure the bulk resistance, reported in Chapters 3 and 4, and those that measure conductivity as a function of time and distance in Chapter 5. A critical review of these various methods was published previously.⁹ In this report the results for four explosives compositions PBX-9404, PBX-9501, PBX-9502, and PBXN-111 are reported. Both sets of experiments share a common electrical circuit which is described below.

BASIC CIRCUIT

The fundamental electrical circuit for all the resistance measurement experiments is shown in Figure 2-1. The main circuit was comprised of a capacitor C , an electrical closing switch, S ; a transmission line inductance and resistance, L_s and r ; and the explosive load inductance and its resistance, L_x and R_x . The capacitor, C , represents the power source. Electrical diagnostics were used to measure the current, i ; the rate of change of current, di/dt ; and the voltage, V . To eliminate contact resistance errors the voltage was measured using a four-probe technique.¹

The switch was either an explosively-activated closing switch,¹⁰ a thyratron, or a triggered spark gap. The switch protected the diagnostic circuits and explosive from prolonged exposure to the electric field. The transmission line was either an array of parallel coaxial cables or a parallel plate stripline.

The choice of circuit components depended on the scale and type of the experiment. The capacitor value ranged from 50 to 1500 μF ; it was charged to the voltage, V_c (2.5 to 40 kV), prior to the start of each experiment.

There are several advantages to using high voltages. First, the contact potentials that exist between the metal electrodes and the conducting explosives, which are typically only a few volts, are too small to affect the high voltage measurements. Second, the large currents that are obtained are well-suited to high speed, high-linearity current measurements using Rogowski¹ coils or current transformers (marked CT in Figure 2-1). Rogowski coils are essentially air-cored current transformers; the output voltage is directly proportional to the rate of change of magnetic flux Φ in the circuit.

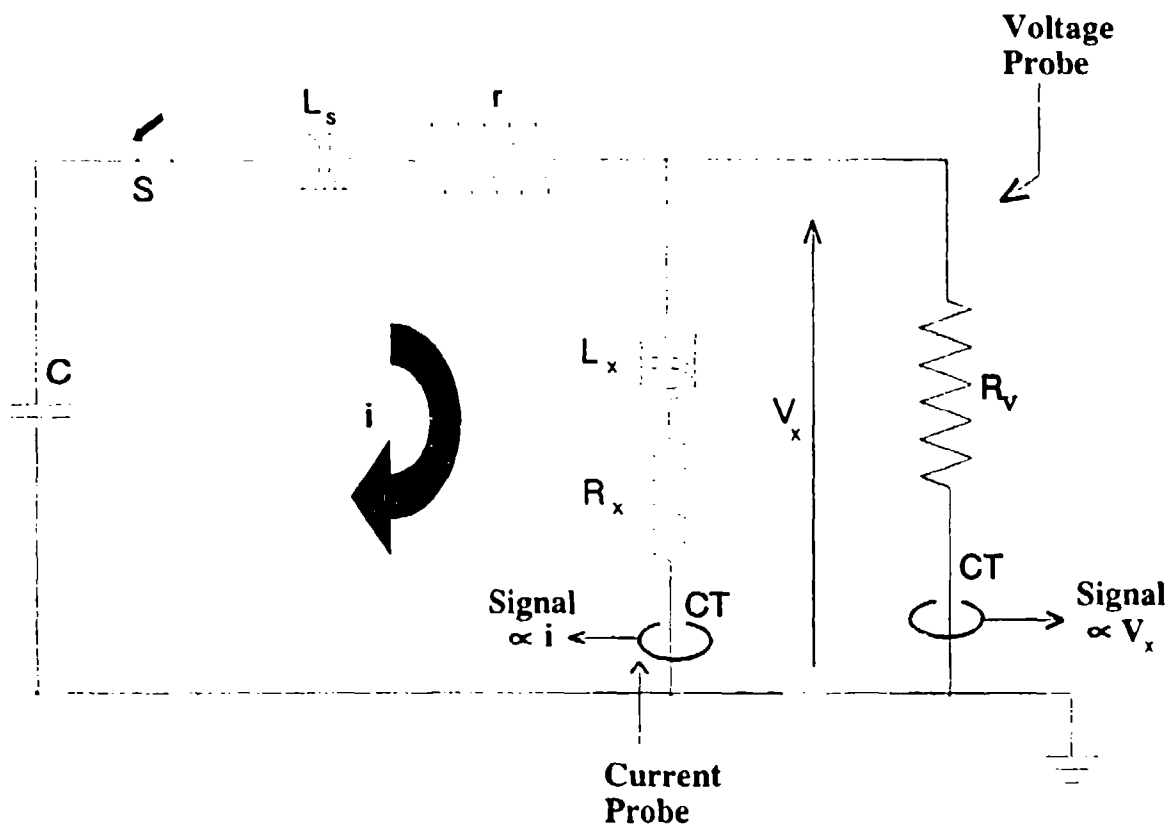


FIGURE 2-1. BASIC CONDUCTIVITY MEASUREMENT CIRCUIT

The capacitor, the transmission line, and the explosive load form a classic LCR series resonance circuit. When the switch is closed the circuit will resonate if it is not sufficiently damped or dissipative. For simplicity we replace the total inductance with L , and the total resistance with R ;

$$R = r + R_x, \quad L = L_s + L_x \quad (2-1)$$

The state of damping is expressed by the quality factor, q . Z_0 is the pulse impedance from classical circuit theory, where

$$Z_0 = \sqrt{\frac{L}{C}}, \quad \text{then} \quad q = \frac{Z_0}{R} \quad (2-2)$$

Using conventional circuit theory we equate the sum of the voltages in the circuit to the voltage on the capacitor, V_c . In this analysis the impedance of the voltage probe, R_v , is considered to be too large to affect the circuit. If time $t = 0$ represents the time when the switch is closed we have

$$\frac{1}{C} \int_0^t i dt + L \frac{di}{dt} + iR = V_c \quad (2-3)$$

The classic solution to this series LCR circuit can be expressed as

$$i(t) = \frac{V_c}{Z_0'} \sin(\omega_0' t) e^{-\frac{R}{2L}t} \quad (2-4)$$

$$\text{where} \quad \omega_0' = \omega_0 \sqrt{1 - \frac{1}{4q^2}}, \quad \omega_0 = \frac{1}{\sqrt{LC}}, \quad q = \frac{\omega_0 L}{R}, \quad (2-5)$$

$$Z_0 = \sqrt{\frac{L}{C}} = \omega_0 L, \quad \text{and} \quad Z_0' = \omega_0' L.$$

Now the voltage across the unknown resistance is iR_x so

$$iR_x = \frac{V_c R_x}{Z_0'} \sin(\omega_0' t) e^{-\frac{R}{2L}t} \quad (2-6)$$

In these experiments the inductance L_x was small, typically less than 1 nH. Small

corrections were made for the voltage across L_x by measuring the inductance prior to the experiment, and then subtracting $L_x di/dt$ from the measured voltage, V_x . (L_x actually diminishes as the detonation wave reduces the length of the current path between the source and the conduction zone; this effect was allowed for by assuming a linear reduction of inductance with time. Reference 1 describes this correction in more detail.)

At the time $t = 0$ the detonation wave, with its conduction zone, enters the electrodes and current i starts to flow. (In other experiments it has been shown that the arrival of the detonation wave shock front is coincident with the start of the conduction zone within 0.5 ns.¹) Consequently, the explosive itself acts as the main closing switch and the voltage $V(t)$ across the explosive becomes:

$$\begin{aligned} V(t) &= V_c - L_s \frac{di}{dt} - r i(t) - \frac{1}{C} \int_0^t i(t) dt \\ &= i(t) R_x + L_x \frac{di}{dt} \end{aligned} \quad (2-7)$$

At $t = 0$, $i(0) = 0$, so

$$\left. \frac{di}{dt} \right|_{t=0} = \frac{V_c}{L} \quad \text{from Equation (2-4)} \quad (2-8)$$

$$\text{and } V(0) = \frac{V_c L_x}{L} \quad \text{from Equation (2-7).}$$

Notice that at $t = 0$ the voltage across the load is independent of R_x because $i = 0$. At that time all the applied voltage appears across the inductances in the circuit. The current then rises approximately sinusoidally and the voltages and currents are recorded. By plotting voltage as a function of current, with the appropriate corrections for $L_x di/dt$, the resistance of the explosive is obtained.

VOLTAGE MEASUREMENTS

It is difficult to measure voltage accurately in explosives experiments because of the rapid changes of current, i.e., $di/dt \geq 10^{10}$ A/s. These errors and their elimination are treated elsewhere.^{1,11} The rapid changes occur due to the short time durations typical of the experiments. Consequently, stray inductances in both the explosive circuits and the voltage probes can cause large errors. Large errors can also arise from the mutual inductances between the explosive's circuit and the voltage probes. These errors are minimized by careful design including the use of parallel striplines. In these experiments, the mutual inductances were reduced to ≤ 1 nH by careful design.

Commercial oscilloscope voltage probes are unsuitable for this work; they are poorly screened from magnetic disturbances and exhibit large errors due to the mutual inductance between the main circuit and the voltage probe circuit. Moreover, the direct connection of the ground wire of a voltage probe invariably produces large errors due to ground loop effects. Ground loops are eliminated by the indirect measurement of current, in a relatively large shunt resistor, R_v , using a current transformer. See Figure 2-1. The resistor, R_v , used here ranged from 100 Ω to 10 k Ω and was made from a solution of copper sulphate (CuSO_4) in a polyethylene tube; details for construction and use of such shunt resistors is given elsewhere.¹

CHAPTER 3

CONDUCTIVITY-DISTANCE DATA OBTAINED
FROM BULK RESISTANCE MEASUREMENTS

The experiments described here were all typified by either a planar or coaxial geometry, in which a high explosive was placed between two metal electrodes; the electrodes extended part-way along the length of the explosive sample. A detonation wave was initiated at one end of the explosive outside the region confined by the electrodes. The detonation wave then entered the explosive between the electrodes so that the velocity vector \underline{D} and the electric field \underline{E} were mutually perpendicular; i.e., \underline{D} was parallel to the length of the electrodes.

The electrodes were connected to a high voltage capacitor bank at a voltage in the range of 2.5 to 40 kV. The explosive acted as a good insulator with a breakdown strength of ≈ 20 kV/mm in its unreacted state; however, when detonating the explosive reaction zone had a conductivity of the order of 100 mhos/m. The detonated explosive thus initiated current flow between the electrodes, and the subsequent electrical current and voltage were monitored as a function of time. By plotting voltage, V , as a function of current, I , i.e., the V - I plot, the dynamic nature of the conduction process was determined.

The resistance R_x of the explosive was then obtained from the slope of the V - I plot. Now in these experiments we could not measure conductivity, $\sigma(x)$, directly but rather the integral of $\sigma(x)$ along the conduction zone. We define a conductivity-zone-width product, $\sigma\Delta$, where Δ was the effective conduction zone width.¹ The $\sigma\Delta$ is an average value, and it is assumed that R_x is constant, then:

$$\sigma\Delta = \int_{-\infty}^{\infty} \sigma(x) dx \quad (3-1)$$

The $\sigma\Delta$ product was then related to R for the two geometries thus:

$$\text{Planar:} \quad \sigma\Delta = \frac{h}{WR_x} \quad (3-2)$$

where h was the explosive thickness and W the electrode width, and

$$\text{Coaxial: } \sigma \Delta = \frac{\ln(r_1/r_2)}{2\pi R_x} \quad (3-3)$$

where r_1 and r_2 were the radii.

The resistance R_x was obtained from the slope of the V-I plot. The plot was typically linear and the line could be extrapolated through the origin. However, a small departure from the line was detected at the time the detonation wave entered the electrodes; this curvature will be discussed in Chapter 5.

COAXIAL EXPERIMENTS

The resistance of the conduction zone in a number of explosives was measured in a coaxial configuration similar to that reported by Demske *et al.*¹² General details of the explosives compositions can be found in the literature.^{5,13}

Each explosive was pushed into a brass or copper tube and a brass electrode was inserted in the center of the explosive; see Figure 3-1. The explosive and the tube were slightly tapered ($1 \mu\text{m}$ diameter per mm length) to insure intimate contact between them. This minimized possible contact resistances, due to air gaps, that can exceed the explosive's resistance.¹¹ The explosives were 127 mm long and detonation was initiated at one end. Two sizes of configuration were used; see Table 3-1.

TABLE 3-1. COAXIAL TUBE DIMENSIONS

Inside diameter (mm)	Outside diameter (mm)	Explosive mass (g)	Tube length (mm)
3.1	14.0	33.0	100.0
11.5	30.2	140.0	75.0

COAXIAL RESULTS

The results of the coaxial experiments are shown in Table 3-2 for both the large (indicated by a †) and small configurations. Typical voltage and current data are shown in Figure 3-2 for PBX-9404. For Figure 3-2 the sequence of events is as follows. Just prior to the time $t = 0 \mu\text{sec}$ the detonation wave enters the space between the coaxial electrodes. When the wave enters current begins to flow and, because of the inductance of the power supply, L , the voltage drops by $L di/dt$, where di/dt is the rate of change of current in the circuit. The voltage across the electrodes is then the sum of the voltage across the explosive's resistance, iR_x ,

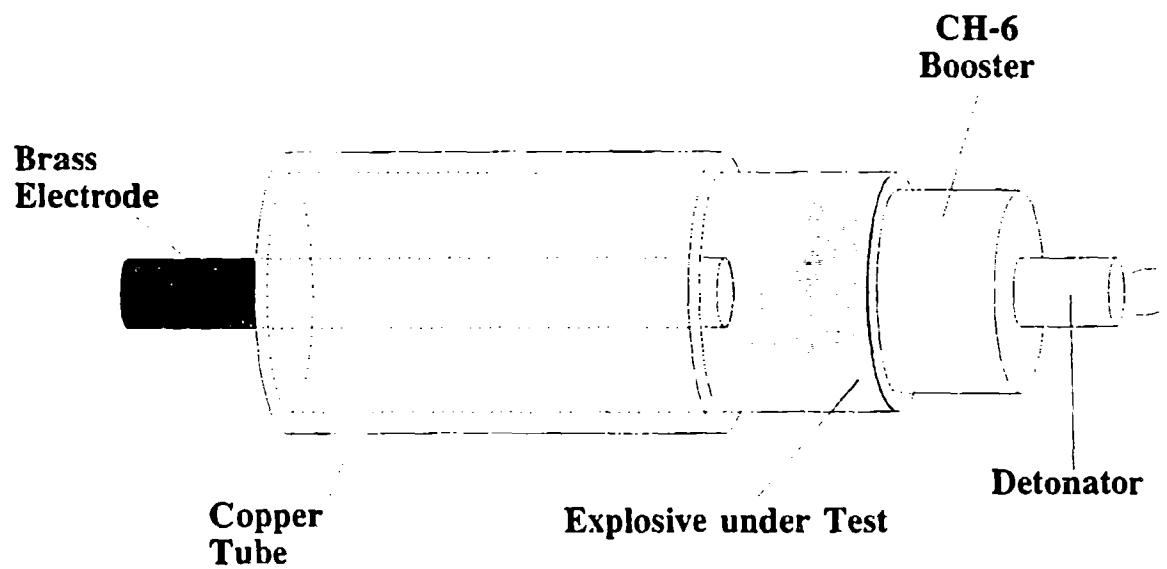


FIGURE 3-1. COAXIAL RESISTANCE MEASUREMENT

and the voltage across the electrode inductance, $L_x di/dt$, as shown in Equations (2-7) and (2-8). By correcting for $L_x di/dt$ the true voltage can be plotted versus the current, so that the resistance may be obtained.

The PBX-9501 results show that $\sigma\Delta$ was independent of charge size. Results suggest that, provided that the explosive's dimensions exceeded the critical diameter, the current flow in the explosive was Ohmic. The explosive performance properties of PBX-9404 and PBX-9501 are virtually identical,⁵ differing only in their sensitivities, so they are usually treated as identical explosives. This is also true for electrical conductivity; no significant differences have been found in this study.

TABLE 3-2. COAXIAL RESISTANCE MEASUREMENTS

Explosive	Resistance R_x (Ω)	$\sigma\Delta$ (mhos)
PBX-9404	0.12 [†]	1.2
PBX-9404	0.20	1.2
PBX-9501	0.20	1.2
PBX-9502	0.02	10.2
PBXW-108	0.12	2.0
PBXW-113(I)	0.09	2.6
[†] Large configuration		

The Effect of a Long Conduction Zone in PBXW-113(I)

The typical V-I plot is linear throughout the duration of the experiment, provided that the explosive's resistance is constant from the beginning of current flow. However, explosives with a long conduction zone clearly take a finite time for that zone to enter the electrodes, and the resistance may take a few microseconds to fall to its final value. Materials like PBXW-113(I) exhibit this type of behavior. The PBXW-113(I) electrical data are shown in Figures 3-3 and 3-4. The data show that the corrections for $L_x di/dt$ did not reduce the initial voltage to zero; it is speculated that this was because of the finite length of the conduction zone in PBXW-113(I). A similar but much shorter duration effect has been observed in PBX-9501; this is described in Chapter 5. The data for PBXW-113(I) show that the resistance does not fall to its final value for $\approx 1.8 \mu s$. Assuming a detonation velocity of $8.39 \text{ mm}/\mu s$ this is equivalent to a conduction zone of $\approx 15 \text{ mm}$ in length.

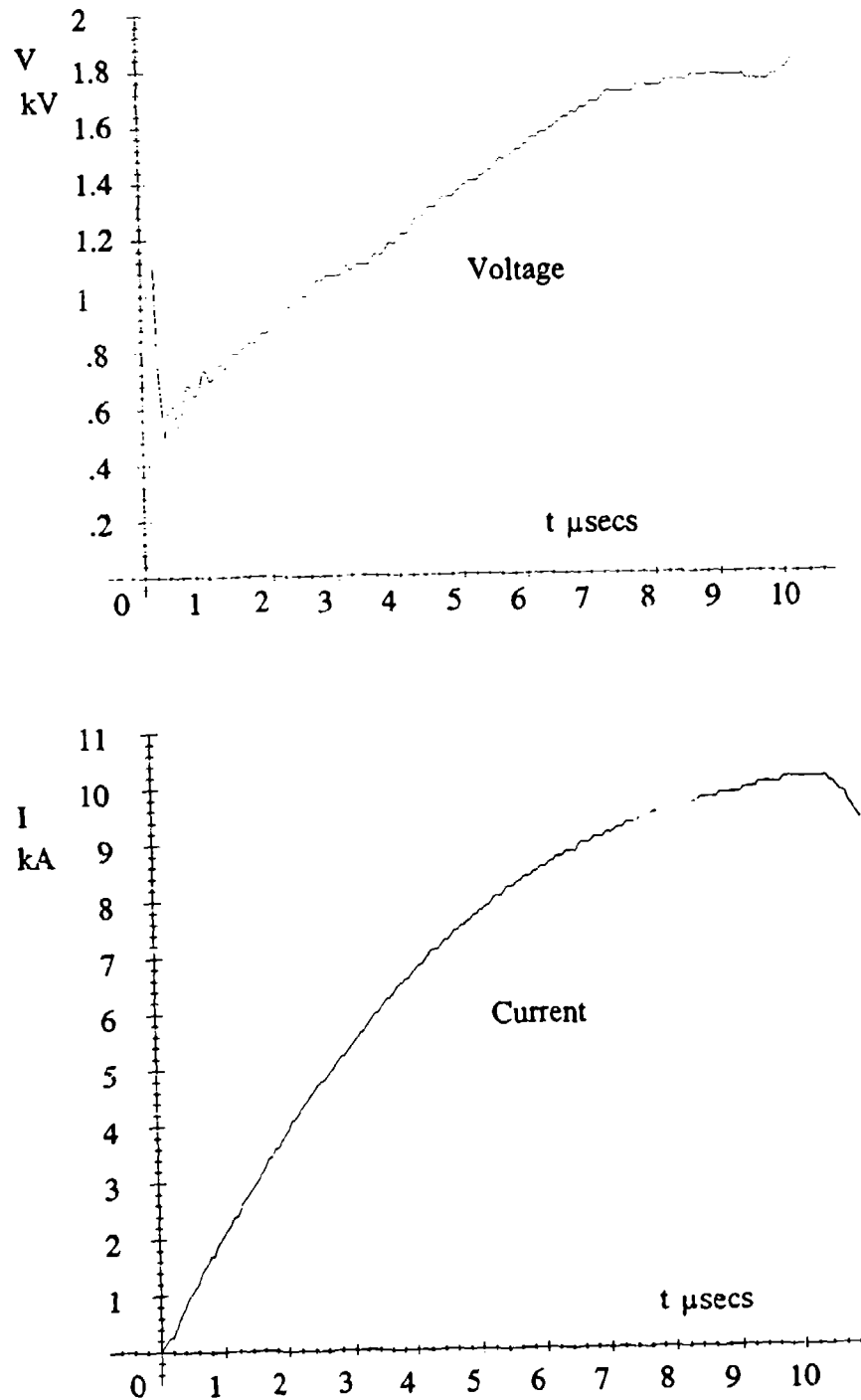


FIGURE 3-2. VOLTAGE AND CURRENT DATA FOR PBX-9404 IN THE COAXIAL EXPERIMENT

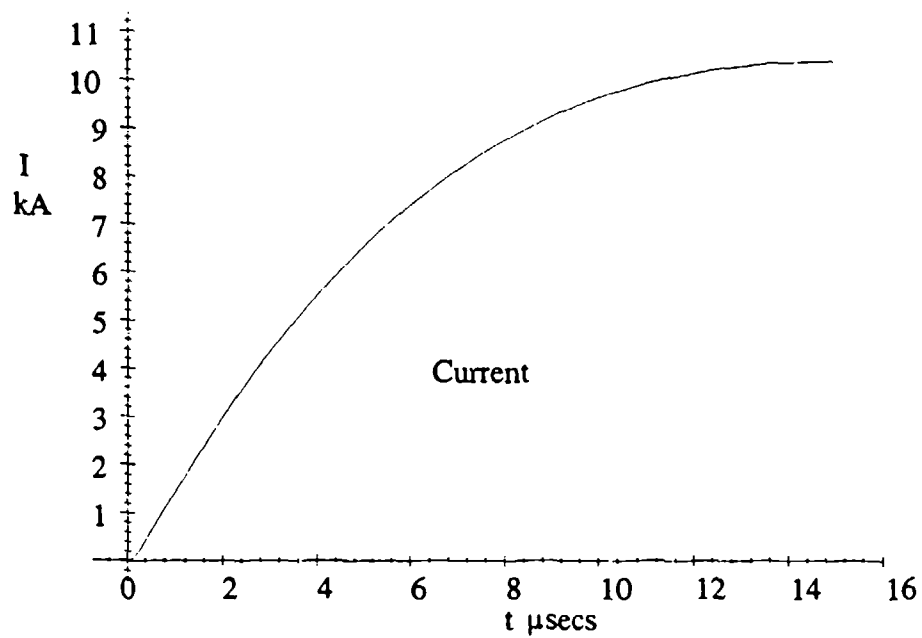
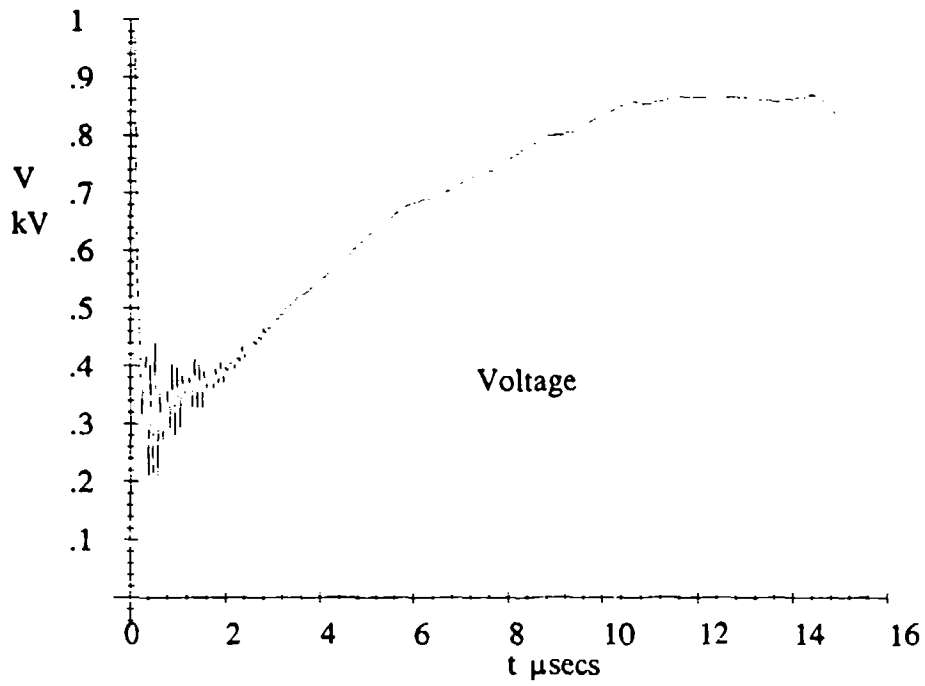


FIGURE 3-3. VOLTAGE AND CURRENT DATA FOR PBXW-113(I) IN THE COAXIAL EXPERIMENT

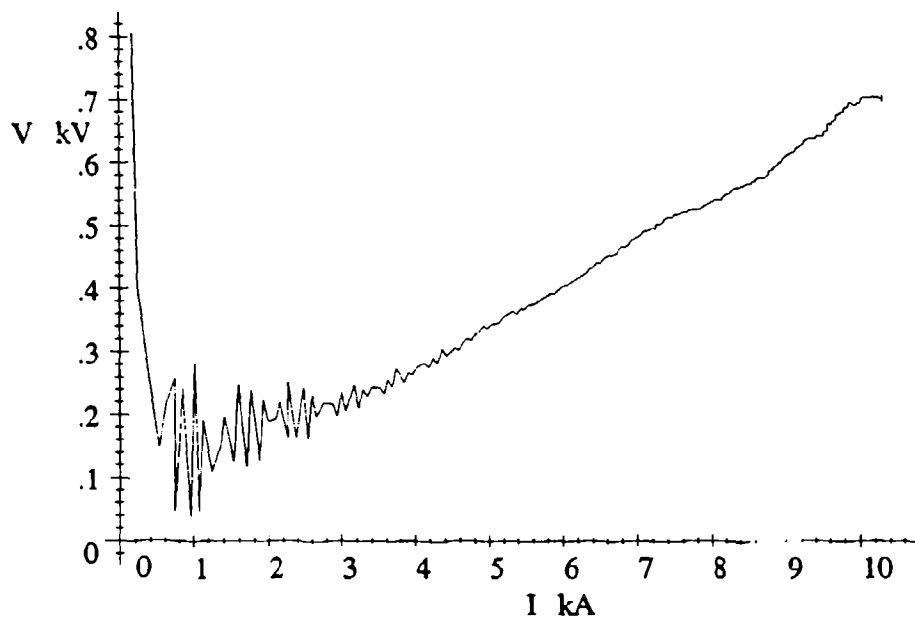
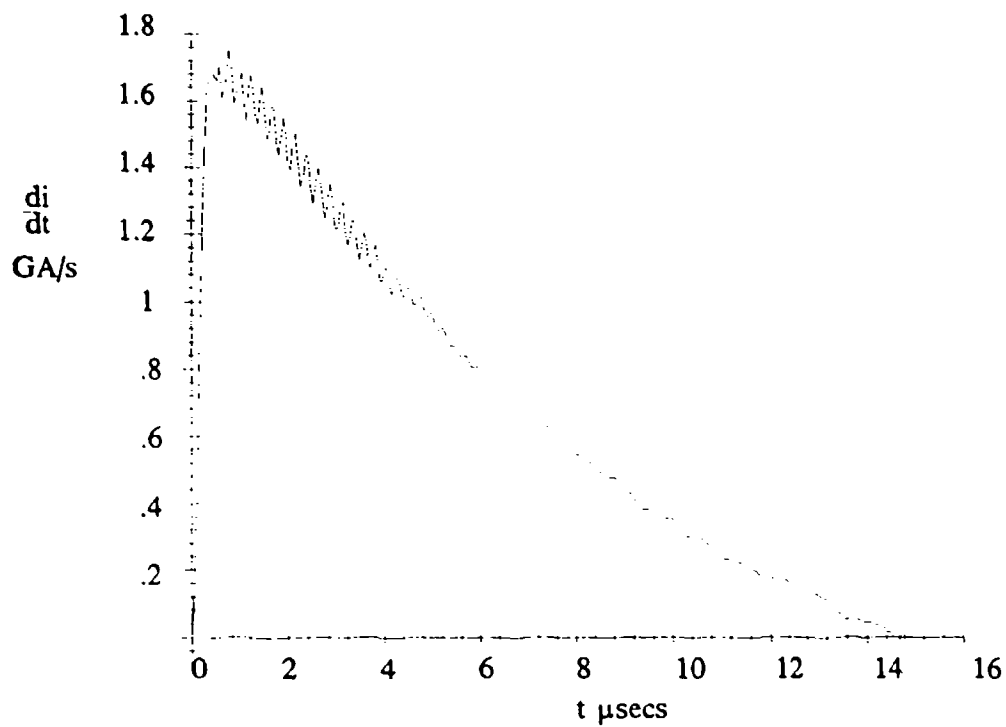


FIGURE 3-4. VOLTAGE VS. CURRENT AND $\frac{di}{dt}$ VS. TIME FOR PBXW-113(I) IN THE COAXIAL EXPERIMENT

PLANAR EXPERIMENTS

The planar experiments were essentially simplified versions of the Ershov experiments described in Chapter 5. A sheet of high explosive was placed between two flat, parallel brass electrodes; see Figure 3-5. A detonation wave was initiated in the explosive sheet with a line wave generator and booster (not shown).

Current and voltage data were measured while the detonation wave travelled along, and parallel to, the electrodes. The electrodes were 12.7 mm wide, 12.7 mm thick, and 150 mm long. The explosives sheets ranged from 1 to 25.4 mm thick.

PLANAR RESULTS AND DISCUSSION

The conductivity zone-thickness products, obtained using Equation (3-2) for the planar experiments, are shown in Table 3-3; for comparison, the measured detonation velocities, D , and the infinite-diameter detonation velocities, D_∞ , are also included. The thicknesses of the explosive sheets are shown as h .

Apparent Inconsistencies Between Coaxial and Planar Results

Voltage vs. time, current vs. time, and voltage vs. current (V-I) data are shown in Figure 3-6 for PBX-9501 in the planar configuration. It is evident that the conductivity results for PBXs 9404 and 9501 are quite different than the results for the coaxial configuration of Table 3-2. In the coaxial experiments the $\sigma\Delta$ products appear to be independent of charge dimensions, but these dimensions are much greater than their critical diameters of ≈ 1 mm. But in the case of the thin sheets there is a clear thickness dependence, probably because these sheets are close to failure. The failure thickness is expected to be half the failure diameter,¹⁴ i.e., ≈ 0.6 mm for PBXs 9404 and 9501 provided that the wave can propagate 15 to 25 times the failure thickness, i.e., ≈ 12 mm.

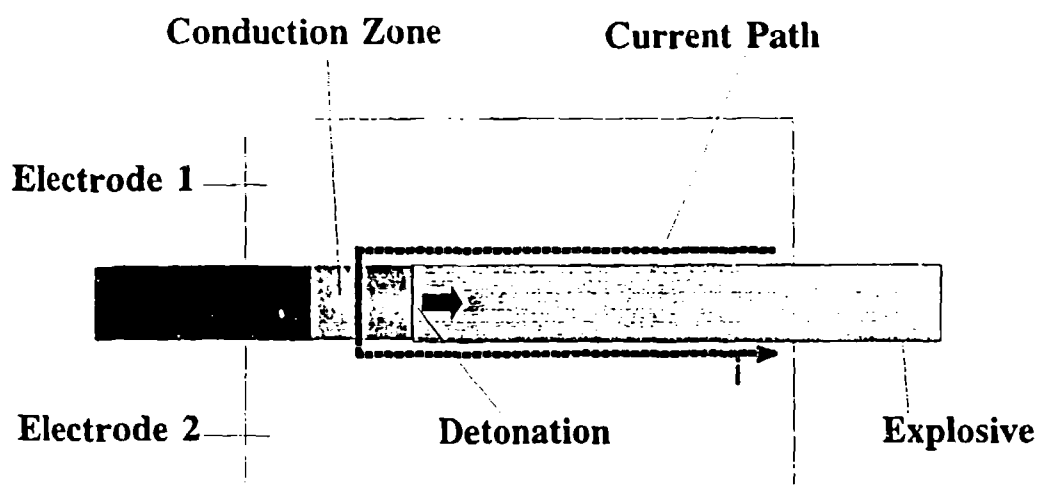


FIGURE 3-5. PLANAR RESISTANCE MEASUREMENT EXPERIMENT

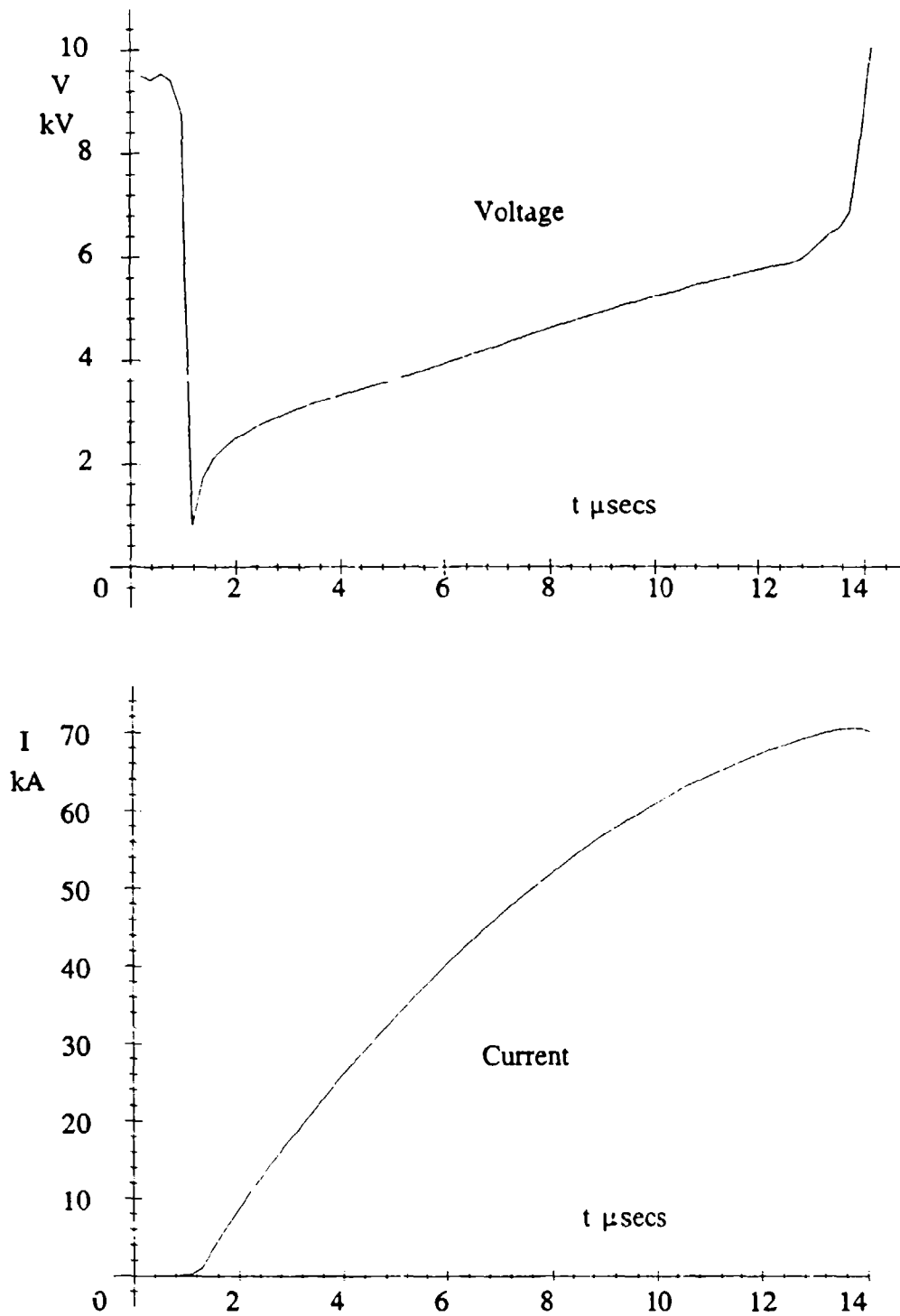


FIGURE 3-6. VOLTAGE AND CURRENT DATA FOR PBX-9501 IN THE PLANAR EXPERIMENT

TABLE 3-3. PLANAR CONDUCTIVITY $\sigma\Delta$ PRODUCTS

Explosive	h (mm)	$\sigma\Delta$ (mhos)	D (mm/ μ s)
PBX-9404 [†]	1.00	0.20	8.30
PBX-9501 [†]	1.00	0.24	8.27
PBX-9501	2.00	0.54	8.52
PBXN-111 ^{††}	12.7	0.20-0.40	5.27
PBXN-111	25.4	0.04-0.40	5.37
[†] D _∞ = 8.82 mm/ μ s ^{††} D _∞ = 6.20 mm/ μ s			

The observed dependance of the $\sigma\Delta$ product on thickness, for explosives sheets close to failure, is clearly an important finding. The results given in Chapter 5 explain these apparent inconsistencies, where the measurement of conductivity in PBX-9501 as a function of time is reported.

Departures from Linearity

Small departures from the linear V-I plots at the beginning of the traces have been detected, i.e., when the detonation wave first entered the electrodes; see Figure 3-4. These effects were first thought to be due to errors in voltage measurement arising from various magnetic effects. In particular, it was believed that the corrections for electrode inductance, $L_e di/dt$, were in error. Despite exhaustive tests these departures could not be eliminated. The true origin of these errors was not identified until time-resolved conductivity measurements were made. The departure was found to be a real physical effect due to the existence of a tail in the conductivity profile; this is described in Chapter 5.

CHAPTER 4

CONDUCTIVITY OF DETONATING ALUMINIZED EXPLOSIVE

The measurement of conductivity may provide valuable insight related to details of the combustion of aluminum in plastic-bonded Navy explosives. The Navy's plastic bonded explosive PBXN-111 studied here contains 25 percent aluminum by weight.

The technique for measuring resistance in aluminized explosives is essentially the same as the measurement in thin sheets of explosive discussed in Chapter 3. Attempts to measure the PBXN-111 conductivity structure using the Ershov experiment were unsuccessful because of the large failure thickness of the explosive compared to the sizes which could be practically used in these experiments.

DETONATION STABILITY IN SHEETS OF PBXN-111

A series of experiments were performed to establish the thickness of PBXN-111 that could sustain a stable detonation. Square slabs of PBXN-111, 75 mm in length and width, were initiated in various thicknesses by PBX-9501 boosters. The results showed that the explosive could be detonated in thicknesses of 12.7 mm or greater if it were confined by heavy brass plates; see Appendix A. The measured failure diameter of PBXN-111 is 37.1 mm,¹⁵ which agrees favorably with our data if a two to one ratio between failure diameter and thickness is assumed.¹⁴ With the benefit of the conductivity results discussed later, it is known that the detonation may have been unstable in these tests, i.e., the wave may not have been fully detonating. These observations are consistent with the calculations by Kennedy which indicate that the chemical reaction of PBXN-111 may be only 12 percent complete at the sonic surface,¹⁶ whereas for an ideal explosive reaction would be complete.

ATTEMPTS TO MEASURE PBXN-111 CONDUCTIVITY VS. TIME

Measurements of PBXN-111 conductivity were attempted using a modified Ershov experiment. In experiments with small failure diameter explosives used in thin, flat sheets, e.g., PBX-9501, the ratio of width, W , to thickness, h , was relatively large, $W/h > 5$. Consequently, errors caused by the divergent fields at the edges of the electrodes were negligible. (We verified this with guard-electrode experiments where the elimination of field divergence had no detectable effect on the measured bulk resistance of PBX-9404.)

Narrow electrodes are necessary for the Ershov experiments because of problems associated with wave curvature, these are described in Chapter 5. The detonation wavefront must be precisely parallel to the slit, or otherwise the measured conductivity profile will be perturbed as the front sweeps across the slit. But the large failure thickness of PBXN-111 caused h to be large and therefore, W/h to be small. Consequently, guard-electrodes were used to eliminate field divergence and to provide confinement; see Figure 4-1.

In this experiment a center electrode, 12.7 mm square cross-section, was used to measure conductivity in a 12.7 mm thick sheet of PBXN-111. Parallel guard-electrodes, 12.7 mm thick and 25.4 mm wide, provided confinement and the elimination of fringe fields. The guard-electrodes were insulated from the center electrode with thin strips of Teflon (PTFE). Rogowski coils, marked RC in Figure 4-1, were used to monitor currents in the center electrode, and all three electrodes combined. The guard-electrodes were connected with heavy copper-braids, and the voltage was measured as described in Chapter 2. Figure 4-1(A) shows how one set of electrodes were configured. Figure 4-1(B) shows how the electrodes were placed above and below the explosive; this view is from the booster end of the explosive, i.e., from the right side of Figure 4-1(A).

It was found that the Teflon insulation was quickly destroyed by the detonation wave; this made it impossible to measure current in the center electrode. Consequently, the Ershov experiments were abandoned for PBXN-111, and simpler bulk resistance measurements using wide, single electrodes were performed.

BULK RESISTANCE MEASUREMENTS IN PBXN-111

The bulk resistance of detonating PBXN-111 was measured in the apparatus shown in Figure 4-2. The explosive was confined by 25.4 mm thick brass plates and initiated by the booster system described above. Prior to detonation an electric field E was applied across the explosive. Unreacted PBXN-111 conducts in electric fields exceeding ≈ 1 kV/mm. Consequently, it was necessary to insulate the explosive with a 25 μ m thick film of Kapton type H (polyimide) insulation. This insulation has a dielectric strength of $\approx 3 \times 10^8$ V/m; however, it conducts readily when shock-loaded above ≈ 5 GPa.¹⁰ The Kapton thus prevented the explosive from conducting and igniting prior to arrival of the detonation wave. When shocked to the detonation pressure, ≈ 12 GPa, the Kapton resistance became negligibly small, hence the true resistance of the explosive could be measured; see Figure 4-2. (A second voltage probe was used to measure the potential difference across the film to verify that the Kapton's resistance was indeed negligible; the probe was connected to a short length of copper foil as shown in Figure 4-2.)

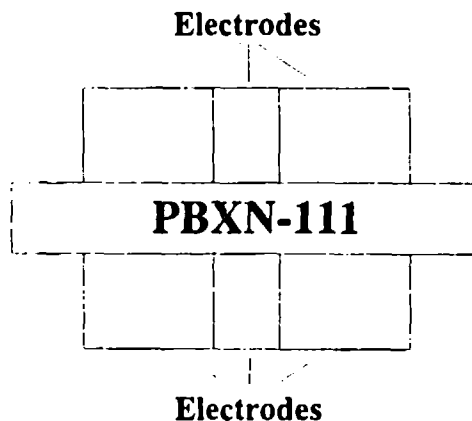
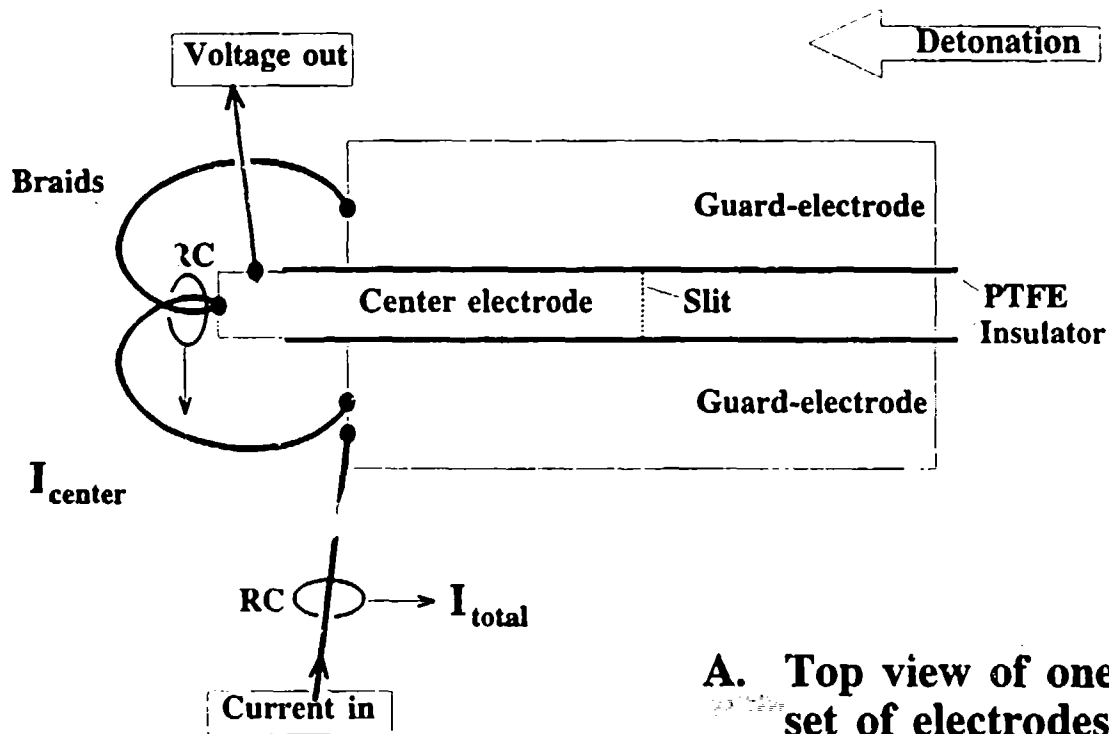


FIGURE 4-1. APPARATUS TO MEASURE CONDUCTIVITY STRUCTURE IN PBXN-111 USING GUARD-ELECTRODES, A. TOP VIEW OF ELECTRODE, B. END VIEW FROM BOOSTER

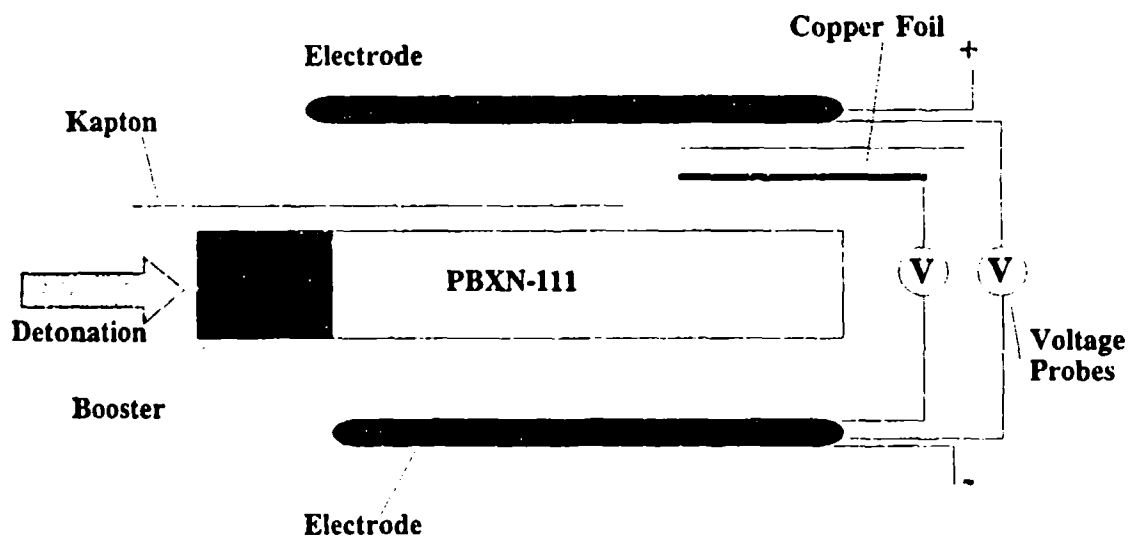


FIGURE 4-2. PBXN-111 RESISTANCE MEASUREMENT APPARATUS, EXPLODED VIEW

PBXN-111 RESULTS AND DISCUSSION

Figure 4-3 shows the measured voltage and current from one experiment performed on 25.4 mm thick PBXN-111. Electrodes of 75 mm width and 150 mm length were used. The initial voltage on the capacitor was 5 kV.

The structure of this current waveform is unusual, perhaps unique; we have not observed it in any other explosives. From ionization pin data the detonation wave took 26 μ s to sweep the length of the electrodes, i.e., it exited the electrodes at 26 μ s, which is off the graph. However, the current rose to 2.9 kA, and then decayed to 500 A within 8 μ s; the decay continued for the remainder of the experiment. Another apparently identical experiment gave different results: the first peak was only 1 kA, followed by a similar decay and then a rapid rise after 10 μ s to 4 kA; see Figure 4-4.

These results were at first interpreted as evidence of late reactions in the explosive. However, there are large variations from experiment to experiment which suggest that the detonations were unsteady and that these strongly affected the measurements. The results are probably due to a combination of variations from experiment to experiment and late reaction effects. It is certain that 25.4 mm thick sheets of PBXN-111 are close to the critical thickness. Therefore, the initial current peak may be due to the over-boosting of the explosive. In the light of these results, the experiments should be repeated with greater lengths of explosive to allow the detonation waves to stabilize prior to the measurements of resistance.

Leiper¹⁷ has analyzed the performance of a 'highly non-ideal explosive' similar to PBXN-111. Using a slightly divergent flow-code he found that less than 70 percent of the formulation reacted within the subsonic part of the flow; even at several times the critical charge diameter, reaction was not complete before the sonic plane. He suggested that a similar effect may account for the results for PBXN-111.

Leiper's findings are certainly in keeping with our anomalous PBXN-111 data. Many other researchers have observed, or suggested, that the detonation process in even ideal explosives requires relatively long distances (many charge diameters) to stabilize. Notable references to these effects include Ramsay,¹⁴ Jones,¹⁶ Mader,¹⁸ and Bdzil.¹⁹ Clearly non-ideal explosives, such as Leiper's, are likely to take even longer to stabilize. Clairmont et al. observed that explosives loaded with ammonium perchlorate (AP) need relatively large length to diameter ratios for detonation to stabilize, they observed a detonation that failed after the wave had travelled 7.5 diameters,²⁰ this is discussed further by Price.²¹ All these effects can be interpreted as evidence of late reactions behind the sonic surface.

The role of aluminum in non-ideal explosives is particularly interesting. The reaction of the aluminum is quite slow; detonation performance data suggest that the energy release takes tens or hundreds of μ s. This reaction should have little effect on the detonation velocity and

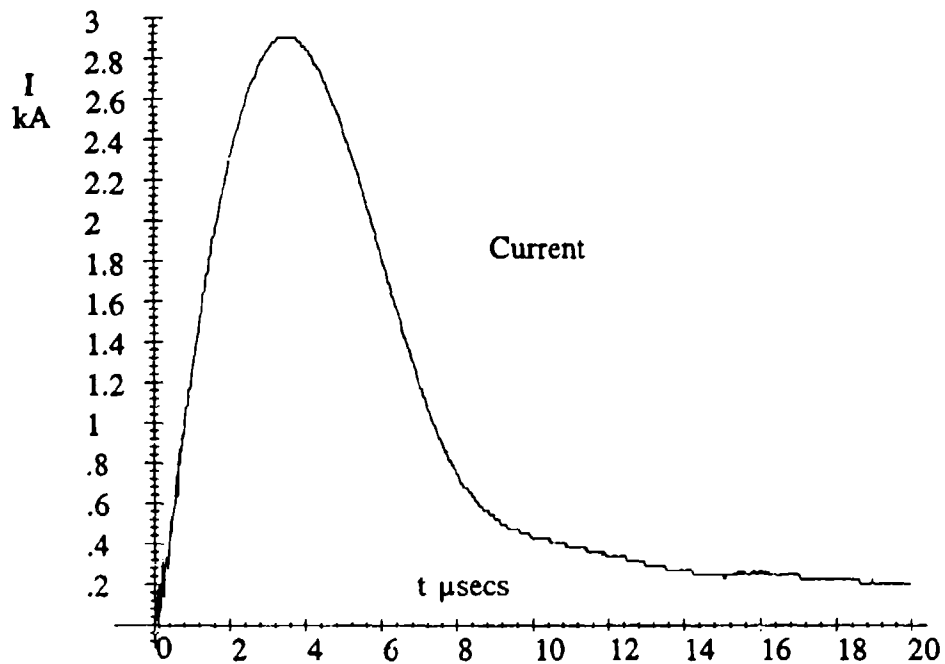
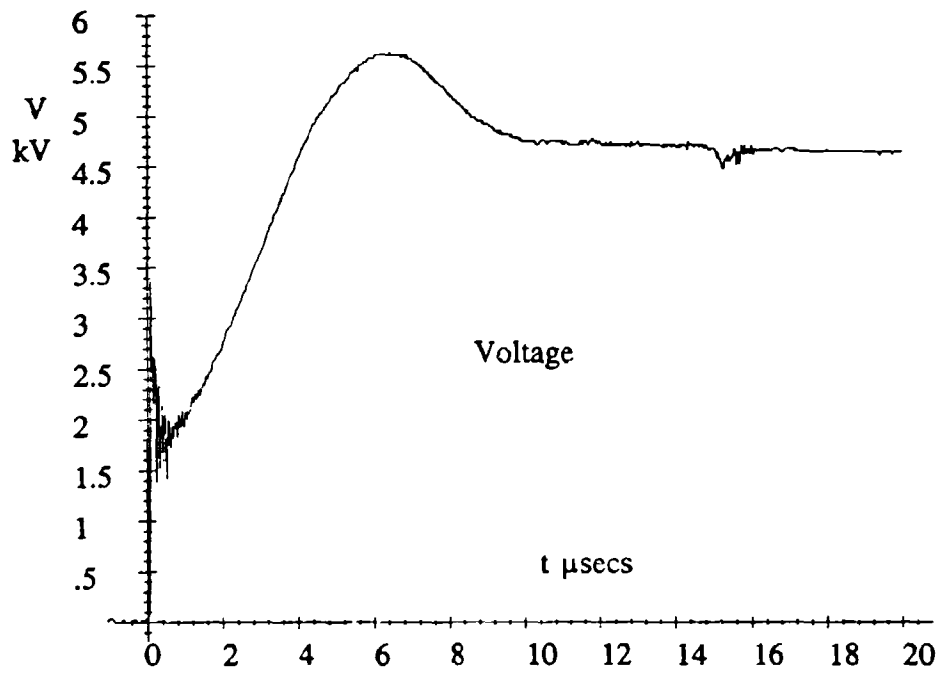


FIGURE 4-3. VOLTAGE AND CURRENT MEASUREMENTS IN DETONATING PBXN-111, FIRST EXPERIMENT

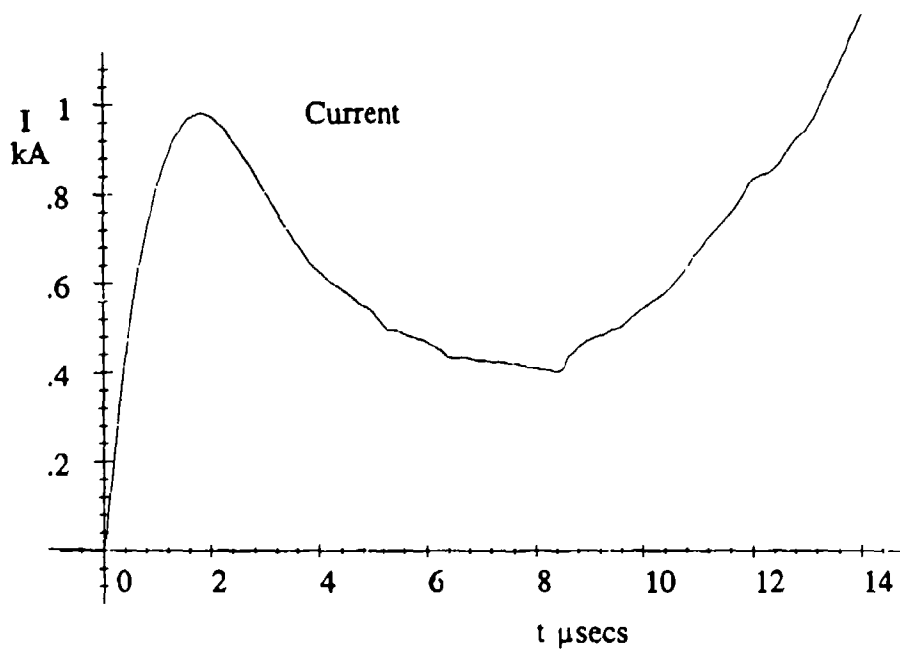
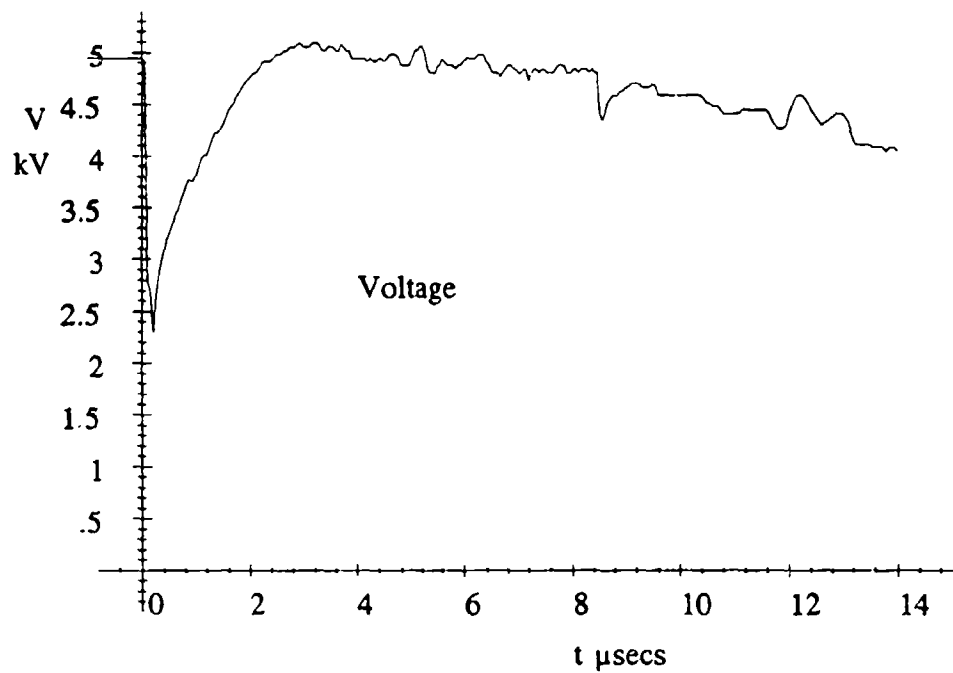


FIGURE 4-4. VOLTAGE AND CURRENT MEASUREMENTS IN DETONATING PBXN-111, SECOND EXPERIMENT

pressure. Yet Akimova²² has observed that the addition of small particle size aluminum to cast TNT compositions actually decreases the failure diameter, and other workers including Gimenez²³ and Price²⁴ have observed the effects of aluminum upon the reactions occurring within as little as 2 μ s of the detonation front. Flückiger observed that the effects of aluminum reaction were observed about 5 μ s after detonation in the cylinder test.²⁵ The results show that the effects of aluminum reaction continue for some time behind the detonation front. Clearly, the electrical conductivity is sensitive to the degree of reaction in PBXN-111 and can therefore be used as a reaction diagnostic.

CHAPTER 5

TIME RESOLVED CONDUCTIVITY MEASUREMENTS

Ershov²⁶ has reported an ingenious technique which can be used to measure conductivity in a plane wave geometry with a near parallel electric field. The technique is capable of providing high time-resolution data; it has been adapted to provide the measurements reported here.

A thin sheet of high explosive was placed between two flat, parallel brass electrodes; see Figure 5-1. A narrow insulated slit was positioned against the explosive in the center of the bottom, ground electrode; a conducting loop bridged the slit in the electrode. A high voltage power supply (not shown) was connected to the electrodes on the right side of the test configuration shown in Figure 5-1. The rate of change of electric current in the loop was measured with a Rogowski coil. Detonation was initiated on the left hand side of the explosive sheet with a line wave generator and booster (also not shown). The detonation wave travelled in a direction perpendicular to the slit, as shown, so that the wave front was parallel to it.

The sequence of sketches in Figure 5-1 shows the progression of the conduction zone from left to right in the explosive. The beginning of the experiment is shown in the top of the figure. The current travelled along the top electrode, down through the conduction zone, along the bottom electrode and around the loop, and then back to the power supply; the Rogowski coil detected the total current, i . Later the conduction zone straddled the slit and current flowed on both sides of it; see the central figure and enlarged version in Figure 5-2(A). Finally, in the bottom of Figure 5-1 the current travelled along the top electrode, down through the conduction zone, along the bottom electrode, and back to the power supply; no current flowed in the loop after passage of the detonation conduction zone.

As Ershov demonstrated, the electric field \underline{E} behind the conduction zone of conductivity, σ , is not perturbed by the current flow, provided that the vectors \underline{E} and $\underline{\text{curl}} \sigma$ are perpendicular. The current density, j , and conductivity, σ , can now be expressed as functions of time, t , for the direction parallel to the applied field E ,

$$j(t) = \sigma(t)E \quad (5-1)$$

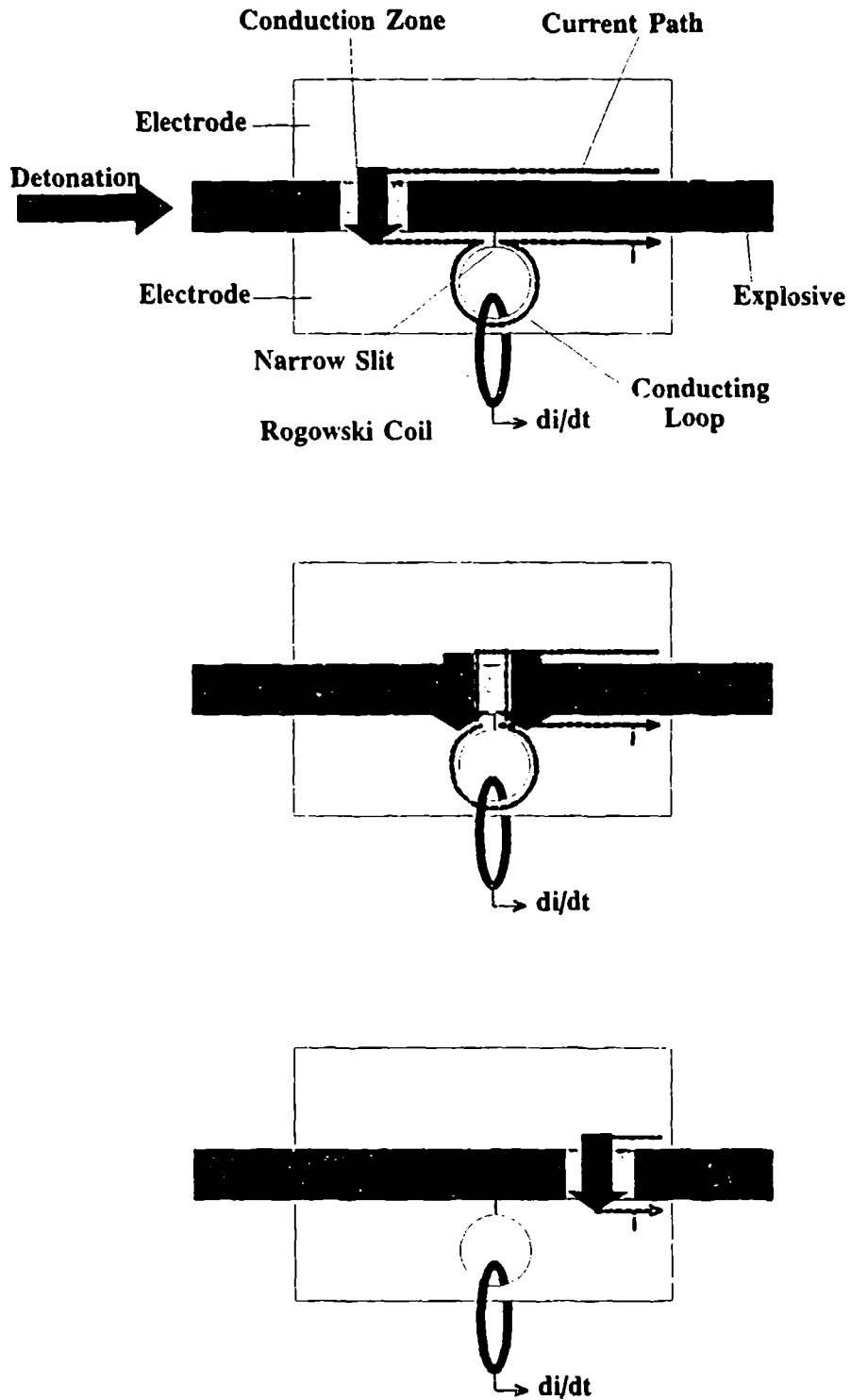


FIGURE 5-1. TIME RESOLVED CONDUCTIVITY EXPERIMENT SHOWING CONDUCTION ZONE MOVING FROM LEFT TO RIGHT

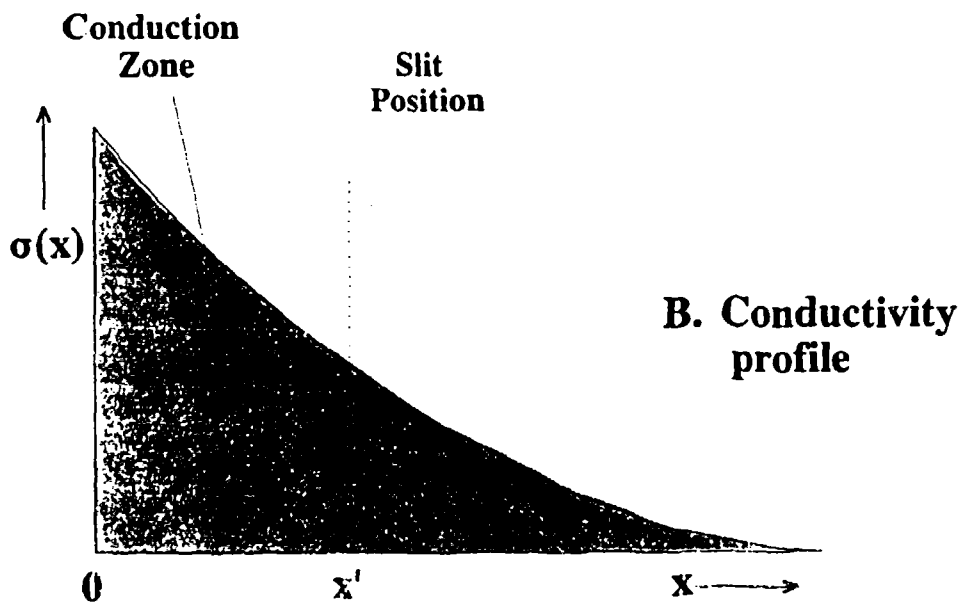
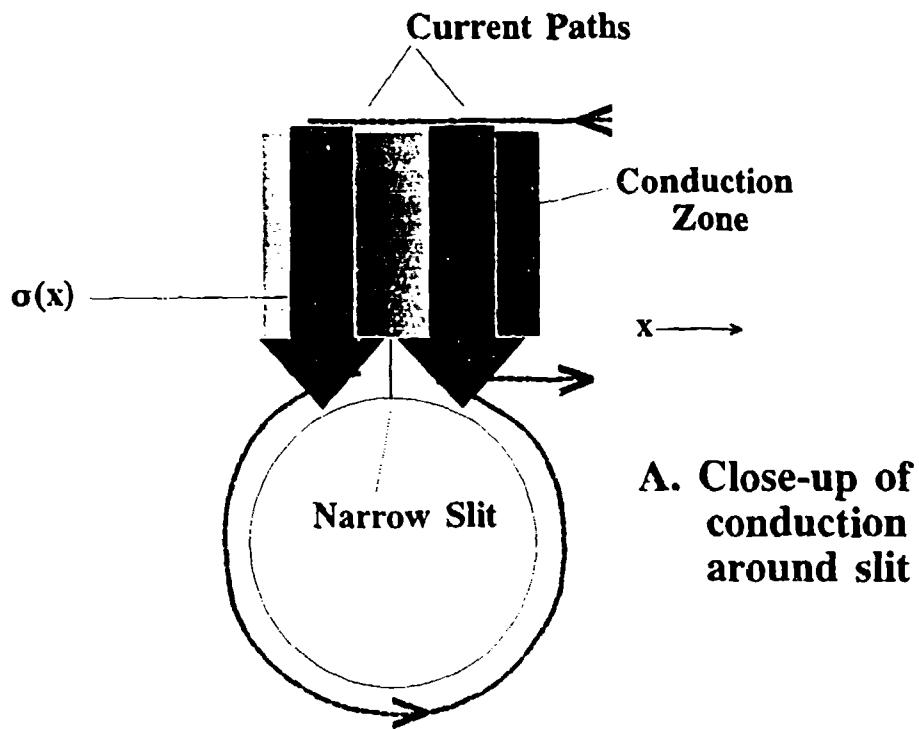


FIGURE 5-2. A. CLOSE-UP OF CONDUCTION PATHS AROUND SLIT
B. CONDUCTIVITY PROFILE ADJACENT TO SLIT

Now $j(t)$ is the current $i(t)$ per unit area. The area of conduction in the direction of \underline{E} is the conductor width W multiplied by the length in the x direction, so

$$i(t) = W \int_0^x E \sigma(x) dx \quad (5-2)$$

The power supply is connected to the ends of the electrodes furthest from the detonator. The wave enters the explosive between the electrodes at $x = 0$ and $t = 0$, and it arrives at the slit at $x = x'$, $t = x'/D$ where D is the detonation velocity; see Figure 5-2(B).

If the field E and the velocity D are independent of distance, x , then the substitution of $x = Dt$ and $E = V/h$ is valid, where V is the voltage between the electrodes, and h is their separation. Then:

$$i(t) = \frac{WDV}{h} \int_0^{\frac{x}{D}} \sigma(t) dt \quad (5-3)$$

$$\frac{di(t)}{dt} = \sigma(t) \frac{WDV}{h} \quad (5-4)$$

The last expression demonstrates the elegance of the Ershov technique: di/dt follows the exact profile of the required quantity, $\sigma(t)$. Moreover, accurate di/dt data are easy to obtain using a Rogowski coil. Since di/dt is directly proportional to $d\Phi/dt$, then the output is also proportional to $\sigma(t)$ from Equation (5-4).

EXPERIMENTAL DETAILS

The explosive sheets were approximately 150 mm square, 1.00 mm or 2.00 mm thick, and extended beyond the edges of the 12.7 mm wide electrodes. A 200 μm wide slit (or gap) was cut across the width of one electrode so that it was parallel to the detonation front and interrupted current flow along the surface of the electrode. A low inductance, low resistance loop maintained current flow around the slit; the $L di/dt$ and iR voltage differences were negligible for this experiment. The loop was formed by a 5.2 mm diameter hole drilled in the electrode at the end of the slit; see Figure 5-1.

The slit was insulated with Teflon film to delay breakdown across the slit. The breakdown could be due to dielectric failure in the slit, or mechanical closure by hydrodynamic flow of the metal electrodes. When such breakdown occurs the current no longer flows in the loop and the di/dt measurement is terminated.

The main electrical circuit is similar to those reported in Chapters 2 and 3 for the planar experiments. The data were recorded on transient digitizers and 1 GHz bandwidth analog oscilloscopes.

A Rogowski coil, with a time resolution of ≤ 1 nsec, was placed in the hole adjacent to the slit to measure the rate of change of current di/dt . To test the validity of the Rogowski coil di/dt data, the records were integrated numerically and compared with independent current data from a calibrated current transformer. The data were in good agreement. For a slit of $200\text{ }\mu\text{m}$ width, the time resolution, given by the detonation transit time across the slit, was 22 ns.

If the detonation front were not straight and parallel to the slit then the resultant di/dt record would be perturbed by this wave structure, i.e., the wave would not cross the slit at all points across its width simultaneously. Measurements of shock wave curvature using a streak camera showed a maximum uncertainty of ≈ 10 ns due to wave curvature.

TIME RESOLVED MEASUREMENTS IN PBX-9501

Conductivity data are shown for 1 mm and 2 mm thick sheets of PBX-9501 in Figure 5-3. Typically the current and voltage at the time of conductivity measurement were 4.0 kA and 1.5 kV. The peak conductivities for both thicknesses were ≈ 220 mhos/m and the durations of the initial conduction spikes were ≈ 100 ns. The initial spikes were followed by lower level, longer duration tails; these tails were markedly different for the two thicknesses.

The data shown in Figure 5-3 for the 2 mm thickness have an abrupt break, at ≈ 900 ns, which was most probably due to closure of the $200\text{ }\mu\text{m}$ slit. When the slit closes current flows across the slit instead of in the loop; such breaks are quite common and unavoidable. Measurements of current and voltage taken at the same time as di/dt confirmed that conduction continued for an additional 1 or 2 μs in the explosive.

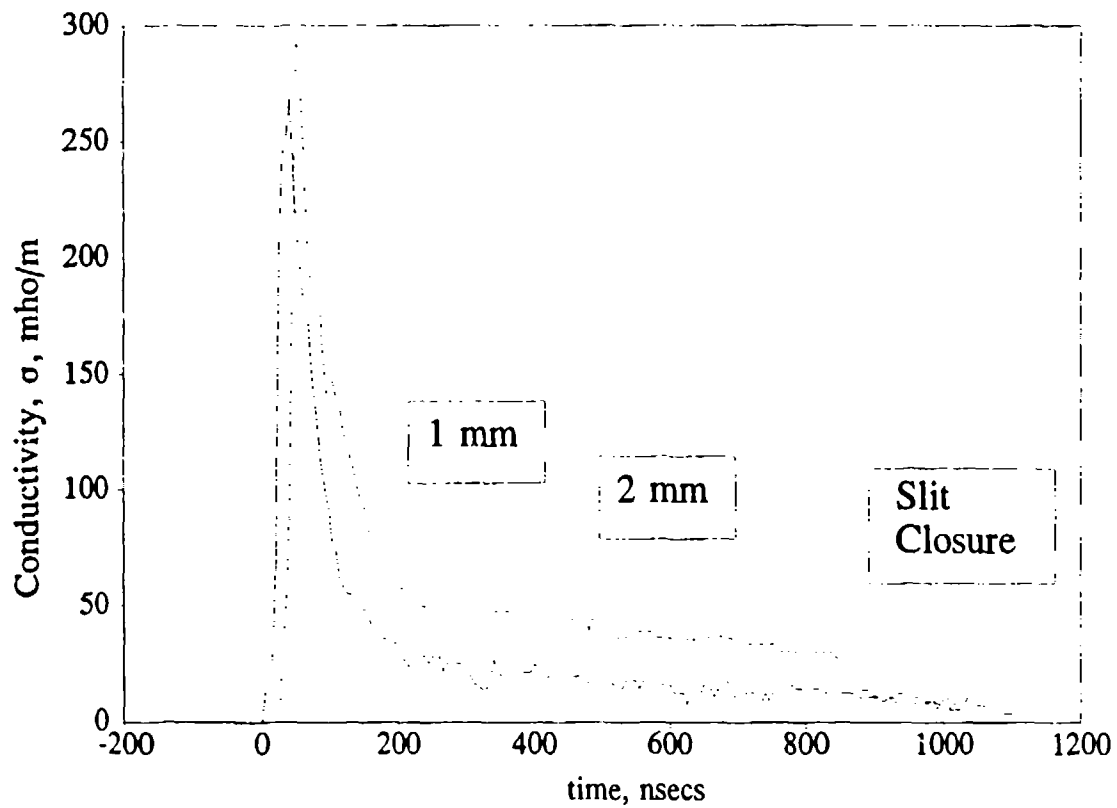


FIGURE 5-3. PBX-9501 CONDUCTIVITY STRUCTURES FOR THICKNESSES OF 1 mm AND 2 mm

CHAPTER 6

DISCUSSION AND CONCLUSIONS

BULK RESISTANCE MEASUREMENTS

From the dynamic resistances of detonating explosives the products of the explosives' conductivities and conduction-zone widths were determined. The V-I plots were typically linear and the lines could be extrapolated through the origin. However, departures from these lines were detected which had occurred at the time the detonation wave first entered the electrodes, i.e., at time $t = 0$, position $x = 0$. These departures were determined to be due to the finite width of the conduction zone. Essentially the electrodes see a conduction zone profile entering from one end. This can be illustrated by estimating the resistance at the beginning of the experiment.

First, we make a simplifying assumption that there is no electric field divergence at the edges of the electrodes. Although this assumption introduces significant errors, it is justified because our purpose is to illustrate the effect of the wave entering the electrodes, not to provide accuracy. (The field divergence could be minimized in the manner described in Chapter 5.) If we combine Equations (3-1) and (3-2) for a planar geometry, and write G for the conductance, i.e., $1/R$, then G can be expressed as

$$G = \frac{1}{R} = \frac{W}{h} \int_0^x \sigma(x) dx \quad (6-1)$$

If we relate distance to time, assuming a steady detonation velocity, D , then $x = Dt$, and we can differentiate to find the rate of change of conductance with time

$$\frac{dG}{dt} = \frac{DW}{h} \sigma(t) \quad (6-2)$$

So, the resistance is constant (and, therefore, the V-I plot is straight) when dG/dt and thus $\sigma(t)$ is zero. This can only occur after the full width of the $\sigma(t)$ profile has entered the electrodes. As was seen for PBXN-111 in Chapter 4, this profile can be tens of microseconds long.

It was generally found that the products of the explosives' conductivities and conduction-zone widths were independent of explosive geometry. However, the results for PBX-9404 and PBX-9501 showed significant differences due to detonation wave instabilities that occur when the explosives' dimensions are close to criticality, i.e., close to failure diameter or thickness.

MEASUREMENTS OF CONDUCTIVITY STRUCTURE

As reported in earlier work the peak conductivity for PBX-9501 was ≈ 220 mhos/m.⁹ The conductivity data reported here have improved time resolution; moreover, the techniques have been refined to observe longer duration structures. The new data show initial spikes in conductivity of ≈ 100 ns duration for all experiments, followed by tails that are strongly dependent on the state of detonation in the explosive. These are believed to be the first published observations of two-step conductivity structures, i.e., a short duration spike followed by a long duration tail.

The conductivity structure of PBX-9501 is particularly interesting. It has been estimated from critical diameter measurements that the reaction zone thickness is approximately $100 \mu\text{m}$,⁵ which is equivalent to a time duration of only 11 ns. Yet the data here show longer than 100 ns conduction spikes followed by at least $1 \mu\text{s}$ -duration tails. Several researchers have noted that their models of detonation phenomena do not adequately match observed data unless a slow-burn term for the combustion of carbon is included.^{6,7,8} Johnson⁷ has suggested that carbon slowly coagulates into large clusters behind the detonation front in the product gases. This coagulation provides an additional, slow energy release after the main reaction. These findings are supported by Hayes' work.⁴

It is estimated that the critical thickness of sheets of PBX-9501 is ≈ 0.6 mm, hence, the propagation of detonation in these 1 mm and 2 mm thick sheets will be influenced by lateral rarefactions. This is confirmed by detonation velocities measured here (8.27 and 8.52 mm/ μs) which are less than published velocities, i.e., 8.83 mm/ μs . Further studies should be done to observe the effects of confinement and explosive thickness.

From this work, it is speculated that the tails of the conduction profiles in PBX-9501 are due to the slow coagulation of carbon in the products. Moreover this coagulation appears to be strongly influenced by the thickness of the explosive sheets. In other words, the arrival of lateral rarefactions, in the wake of the reaction zone, perturbs the coagulation process. The spikes are unaffected because they occur too rapidly. Therefore, detonation failure may be due to the control of the energy release during carbon coagulation in the tail. The measurement of conductivity may be the only way of observing these phenomena.

ALUMINIZED EXPLOSIVE PBXN-111

The aluminized explosives data show the conductivity measurement to be a valuable tool for the analysis of reaction and wave stability during detonation. The results, discussed in Chapter 4, suggest that the structure of the conductivity profile is strongly affected by detonation wave instabilities. The results are probably due to a combination of wave instabilities and late reaction effects. This technique should lead to the formulation of better metallized explosives.

REFERENCES

1. Tasker, D.G., *The Properties of Condensed Explosives for Electromagnetic Energy Coupling*, NSWC TR 85-360, Oct 1985, NSWC, White Oak, Maryland.
2. Crawford, O.H., "Electrical Conductivity in the Reaction Zone of High Explosives," Oak Ridge National Laboratory, May 1985, private communication.
3. Griem, H.R., "Properties of Dense Plasmas Generated by Discharges Behind Shock Waves," University of Maryland, Laboratory for Plasma and Fusion Energy Studies, College Park, MD, Final Report, 28 Jul 1986 - 28 Jul 1987.
4. Hayes, B., "On Electrical Conductivity in Detonation Products," *Proceedings of the Fourth Symposium (International) on Detonation*, Office of Naval Research, Washington D. C., Oct 1965, p. 595.
5. Dobratz, B.M., *LLNL Explosives Handbook*, UCRL-52997, 16 Mar 1981, Lawrence Livermore National Lab.
6. Mader, C.L., *Numerical Modeling of Detonations*, Univ. California Press, 1979.
7. Johnson, J.D., "Carbon in Detonations," in *Proceedings of the 1989 APS Topical Conference in Condensed Matter*, Elsevier Science Publishers, B. V., 1992, p. 697.
8. Tang, P.K., "A Study of Detonation Processes in Heterogeneous High Explosives," *J. Appl. Phys.*, Vol. 63, 1988, p. 1041.
9. Tasker, D.G., Granholm, R.H. and Lee, R.L., "The Fast Measurement of Electrical Conductivity Structure Within The Detonation Zone of a Condensed Explosive," in *Shock Waves in Condensed Matter*, Elsevier Science Publishers, B.V., 1988, p. 923.
10. Tasker, D. G., Lee, R. J., and Gustavson, P.K., *An Explosively-Actuated Electrical Switch Using Kapton Insulation*, NSWCDD/TR-92/124, Feb 1992, NSWCDD, Silver Spring, MD.
11. Tasker, D.G. and Lee, R.J., "High Current Electrical Conduction of Pressed Condensed Detonating Explosives," *Shock Waves in Condensed Matter*, Plenum Publishing Corporation, 1986.

12. Demske, D.L., Forbes, J.W., and Tasker, D.G., "High Current Electrical Resistance of PBX-9404," *Shock Waves in Condensed Matter-1983*, Elsevier Science Publishers B.V., 1984.
13. Hall, T.N. and Holden, J.R., *Navy Explosives Handbook, Explosion Effects and Properties--Part III. Properties of Explosives and Explosive Compositions*, NSWC MP 88-116, NSWC, White Oak, MD.
14. Ramsay, J.B., "Effect of Confinement in 95 TATB/5 KEL-F, *Proceedings of the Eighth Symposium (International) on Detonation*, Albuquerque, NM, Jul 1985, p.372.
15. Forbes, J.W., Lemar, E.R. and Baker, R.N., "Detonation Wave Propagation in PBXW-115," *Ninth Symposium (International) on Detonation*, OCNR 113291-7, Portland, Oregon, 1989, 8.806.
16. Jones, D.A. and Kennedy, D.L., *Application of the CPex non-ideal explosive model to PBXW-115*, Materials Research Laboratory Report MRL-TR-91-40, Oct 1991.
17. Leiper, G.A., discussion of paper by Tasker, D.G. and Lee, R.J., "The Measurement of Electrical Conductivity in Detonating Condensed Explosives," *Ninth Symposium (International) on Detonation*, OCNR 113291-7, Portland, Oregon, 1989, p.405.
18. Mader, C.L., "Chemistry of Build-Up of Detonation Wave," *Actes du Symposium International sur le Comportement des Milieux Denses sous Hautes Pressions Dynamiques*, Commissariat a l'energie atomique, Paris, 1978.
19. Bdzil, J.B., Fickett, W., and Stewart, D.S., "Detonation Shock Dynamics: A New Approach to Modeling Multi-Dimensional Detonation Waves," *Ninth Symposium (International) on Detonation*, OCNR 113291-7, Portland, Oregon, 1989, p.730.
20. Clairmont, A.R., Jaffe, I. and Price, D., *The Detonation Behavior of Ammonium Perchlorate as a Function of Charge Density and Diameter*, NOLTR 67-71, 20 Jun 1967, NSWC, White Oak, Maryland, p.20.
21. Price, D., *Review of Information on Composite Explosives: IV*, ATR-TR-90-35, Aug 1990, Advanced Technology and Research Corporation, Maryland.
22. Akimova, L.N. and Stesik, L.N., "Detonation Capacity of Perchlorate Explosives," *Combustion, Explosion and Shock Waves*, Vol. 12, 1976, p.247.
23. Gimenez, P. et al., "F.P.I. Velocimetry Technique ...," *Ninth Symposium (International) on Detonation*, OCNR 113291-7, Portland, Oregon, 1989, p.1371.
24. Price, Donna, *Review of Information on Composite Explosives: I. General Background*, ATR-TR-88-0046, Nov 1988, Advanced Technology and Research Corporation, Maryland, pp.1-2.

25. Flückiger, R., "Characterization and Performance Tests of Hexals," *Proc. Int. Symp. Pyro. and Expls.*, Beijing, 1987, pp.270-275.
26. Ershov, A.P., Zubkov, P.I. and Luk'yanchikov, L.A., "Measurements of the Electrical Conductivity Profile in the Detonation Front of Solid Explosives," *Combustion, Explosion and Shock Waves*, Vol. 10, No. 6, 1974, p.776.

APPENDIX A

THE VERIFICATION OF DETONATION IN SHEETS OF PBXN-111

EXPERIMENT

These tests were conducted to verify that detonation could be sustained in the thicknesses of PBXN-111 used in the planar conductivity studies; see Chapter 4. Four experiments were performed to determine the thickness required for stable detonation in rectangular slabs of PBXN-111. Figure A-1 illustrates the basic configuration for the experiments. The configurations for each test are shown in Table A-1. The 50.8 mm thick charge was made from two 25.4 mm charges. The confinement was comprised of 76.2 mm square, 12.7 mm thick brass plates placed against the top and bottom faces of the confined test charge, as shown in Figure A-1.

TABLE A-1. TEST CONFIGURATIONS AND RESULTS

Thickness (mm)	Conditions	Dent (mm)
12.7	No confinement	0.00
12.7	Confined	2.54
25.4	No confinement	1.55
50.8	No confinement	3.30

The initiation system consisted of a 114.3 mm wide, 25.4 mm long, 12.7 mm thick PBX-9501 booster and a 1.27 mm thick triangular Detasheet linewave generator. The linewave generators were cut into equilateral triangles, 76.2 mm on a side, from larger linewave generators. A 63.6 mm thick steel witness plate was used to detect detonation at the edge of the PBXN-111 slab furthest from the booster.

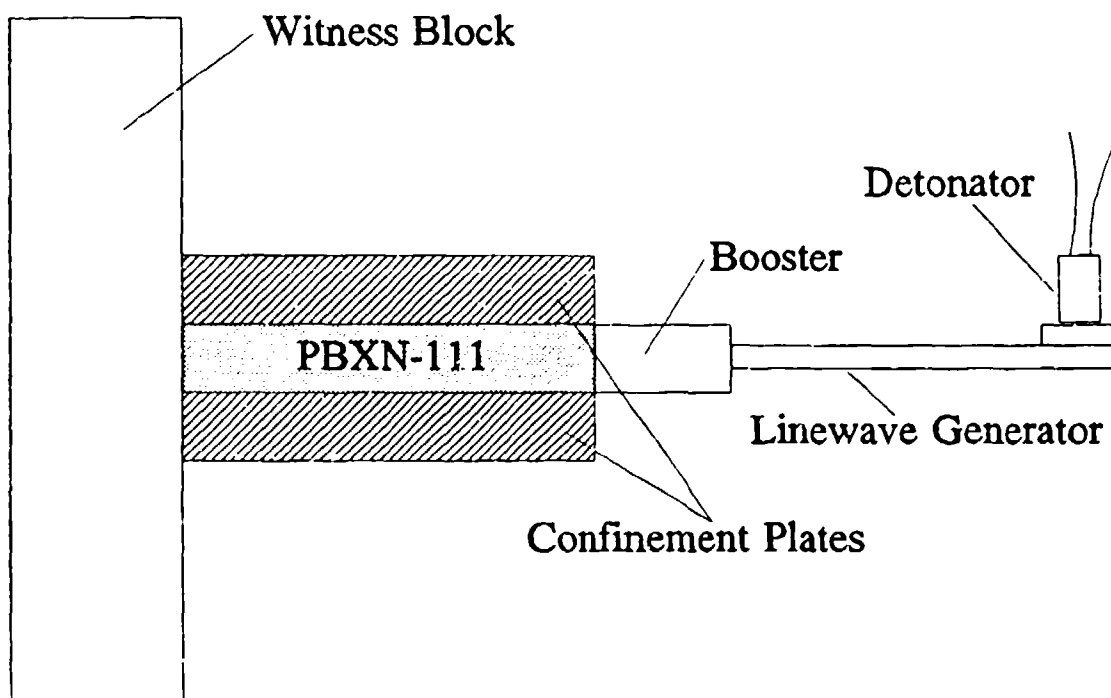


FIGURE A-1. DETONATION VERIFICATION EXPERIMENT

RESULTS

The 12.7 mm thick charge with no confinement was the only configuration that did not detonate. This configuration produced very little indentation in the witness plate and several pieces of the explosive were recovered after the shot. The other experiments produced dent depths of 1.55 mm, 2.54 mm, and 3.3 mm as shown in Table A-1.

CONCLUSIONS

The steel witness block data showed that the explosive could be detonated in thicknesses of 12.7 mm (or greater) using the brass confinement. This configuration was used for the studies described in Chapter 4.

DISTRIBUTION

	<u>Copies</u>		<u>Copies</u>
ATTN ONR(S) 1132P (R MILLER)	1	ATTN 6-A-145	1
ONR(T) 20T (L V SCHMIDT)	1	DDESB-KT	1
ONR(T) 213 (D SIEGEL)	1	J WARD	1
ONR(T) 23 (A J FAULSTICH)	1	CHAIRMAN	
ONR(T) 232 (D HOUSER)	1	DEPARTMENT OF DEFENSE EXPLOSIVES	
CHIEF OF NAVAL RESEARCH		SAFETY BOARD	
800 N QUINCY STREET BCT 1		HOFFMAN BUILDING 1	
ARLINGTON VA 22217-5000		2461 EISENHOWER AVENUE	
		ALEXANDRIA VA 22331	
ATTN R SIEWART	1	ATTN OP-098	1
OUSDRE/R&AT-MST		OP-981	1
THE PENTAGON		OP-982	1
WASHINGTON DC 20301		OP-983	1
		OP-987	1
ATTN D ANDERSON	1	OP-02T	1
OUSDRE/TWP-NW&M		OP-22	1
THE PENTAGON		OP-225	1
WASHINGTON DC 20301		OP-32	1
		OP-35	1
ATTN G KOPCSAK	1	OP-37	1
USDRE/TWP--OM		OP-374	1
THE PENTAGON		OP-501	1
WASHINGTON DC 20301		OP-502	1
		OP-503	1
ATTN F MENZ	1	OP-72	1
USD(A)/DDRE (R/AT/ET)		OP-74	1
STAFF SPECIALIST FOR WEAPONS		OP-75	1
TECHNOLOGY		CHIEF OF NAVAL OPERATIONS	
THE PENTAGON		NAVY DEPARTMENT	
WASHINGTON DC 20301		WASHINGTON DC 20350	
ATTN SURFACE WARFARE	1	ATTN SPAWAR-05	1
AIR WARFARE	1	COMMANDER	
SUBS/ASW	1	SPACE AND NAVAL WARFARE SYSTEMS	
OASN/RE&S		COMMAND	
NAVY DEPARTMENT		WASHINGTON DC 20363-5100	
WASHINGTON DC 20301			

DISTRIBUTION (Cont.)

	<u>Copies</u>		<u>Copies</u>
ATTN SEA-05R	1	ATTN CODE 177	1
SEA-55	1	TECHNICAL LIBRARY	1
SEA-55X	1	COMMANDER	
SEA-55X1	1	DAVID TAYLOR RESEARCH CENTER	
SEA-55X2	1	PORTSMOUTH VA 20375	
SEA-55Y	1		
SEA-66U	1	ATTN TECHNICAL LIBRARY	1
SEA-62	1	COMMANDING OFFICER	
SEA-62Y	1	NAVAL RESEARCH LABORATORY	
SEA-62Z	1	WASHINGTON DC 20375	
SEA-63	1		
SEA-63D	1	ATTN TECHNICAL LIBRARY	1
PMS-402	1	COMMANDING OFFICER	
PMS-406	1	NAVAL SURFACE WARFARE CENTER	
PMS-407	1	DAHLGREN DIVISION	
COMMANDER		COASTAL SYSTEMS STATION	
NAVAL SEA SYSTEMS COMMAND		PANAMA CITY FL 32407-5000	
WASHINGTON DC 20362-5105			
		ATTN TECHNICAL LIBRARY	1
ATTN AIR-5004	1	COMMANDER	
AIR-51623	1	NAVAL UNDERSEA WARFARE CENTER	
AIR-540	1	DIVISION	
AIR-5404	1	NEWPORT RI 02841-5047	
AIR-93	1		
AIR-932F	1	ATTN CODE 3917	1
AIR-932H	1	CODE 38 (R DERR)	1
AIR-932K	1	CODE 389 (T BOGGS)	1
AIR-932T	1	CODE 32	1
PMA-242	1	CODE 3205	1
TECHNICAL LIBRARY	1	CODE 3208	1
COMMANDER		CODE 326	1
NAVAL AIR SYSTEMS COMMAND		CODE 3261	1
WASHINGTON DC 20361		CODE 3263	1
		CODE 3264	1
ATTN TECHNICAL LIBRARY	1	CODE 3265	1
CODE 17	1	CODE 3266	1
CODE 172	1	CODE 327	1
CODE 1740.3 (R GARRISON)	1	CODE 381	1
CODE 1740.4 (S WANG)	1	CODE 385	1
CODE 175 (W SYKES)	1	CODE 3850	1
CODE 1750.2 (W CONLEY)	1	CODE 3853	1
CODE 1740.2 (F FISCH)	1	CODE 3891 (J COVINO)	1
COMMANDER		CODE 39	1
NAVAL SURFACE WARFARE		TECHNICAL LIBRARY	1
CENTER		COMMANDER	
CARDEROCK DIVISION		NAVAL AIR WARFARE CENTER	
BETHESDA, MD 20084		WEAPONS DIVISION	
		CHINA LAKE CA 93555-6001	

DISTRIBUTION (Cont.)

	<u>Copies</u>		<u>Copies</u>
ATTN CODE 2730D	1	ATTN CODE 2145	1
TECHNICAL LIBRARY	1	COMMANDER	
J CHANG	1	PACIFIC MISSILE TEST CENTER	
P DENDOR	1	POINT MUGU CA 93042	
L NEWMAN	1		
COMMANDER		COMMANDING OFFICER	
NAVAL SURFACE WARFARE CENTER		SEAL TEAM 2	
INDIAN HEAD DIVISION		FPO NEW YORK NY 09501-4633	1
INDIAN HEAD MD 20640-5000			
		COMMANDER	
ATTN TECHNICAL LIBRARY	1	NAVAL UNDERSEA WARFARE DIVISION	
COMMANDER		KEYPORT WA 98345-0580	1
CENTER FOR NAVAL ANALYSES			
2000 SUTTLAND ROAD		COMMANDER	
WASHINGTON DC 20390-5140		NAVAL SURFACE WARFARE CENTER	
		PORT HUENEME DIVISION	1
ATTN LIBRARY	1	PORT HUENEME CA 93043-5007	
SUPERINTENDENT			
NAVAL POSTGRADUATE SCHOOL		COMMANDER	
MONTEREY CA 93940		NAVAL WEAPONS EVALUATION	
		FACILITY	
ATTN TECHNICAL LIBRARY	1	KIRTLAND AIR FORCE BASE	
PRESIDENT		ALBUQUERQUE NM 87117	1
NAVAL WAR COLLEGE			
NEWPORT RI 02841		ATTN CODE 3031 (E NEAL)	1
		CODE 50D (A NORRIS)	1
ATTN RDT OFFICER	1	CODE 505 (J E SHORT)	1
SEAL TEAM	1	CODE 90 (A E WHITNER)	1
UNDERWATER DEMOLITION		COMMANDER	
TEAM	1	NAVAL SURFACE WARFARE CENTER	
COMMANDING OFFICER		CRANE DIVISION	
NAVAL AMPHIBIOUS BASE		CRANE IN 47522-5000	
CORONADO			
SAN DIEGO CA 92155		ATTN CODE 321 (M BUCHER)	1
		COMMANDING OFFICER	
ATTN RDT OFFICER	1	NAVAL WEAPONS STATION	
COMMANDING OFFICER		CONCORD CA 94520-5000	
NAVAL AMPHIBIOUS BASE			
LITTLE CREEK		ATTN CODE 470A	1
NORFOLK VA 23511		LIBRARY	1
		OFFICER IN CHARGE	
ATTN TECHNICAL LIBRARY	1	NAVAL SURFACE WARFARE CENTER	
COMMANDING OFFICER		INDIAN HEAD DIVISION	
NAVAL EXPLOSIVE ORDNANCE		YORKTOWN DETACHMENT	
DISPOSAL TECHNOLOGY CENTER		YORKTOWN VA 23691-5110	
INDIAN HEAD MD 20640			

DISTRIBUTION (Cont.)

	<u>Copies</u>		<u>Copies</u>
ATTN TECHNICAL LIBRARY	1	ATTN CHIEF DOCUMENTS	1
DIRECTOR		D DREITZLER	1
DEFENSE NUCLEAR AGENCY		REDSTONE ARSENAL ARMY MISSILE	
WASHINGTON DC 20305		COMMAND	
		REDSTONE ARSENAL AL 35809	
ATTN C FOWLER	1		
DEFENSE SCIENCE BOARD		ATTN SLC-BR-TB-EE	1
THE PENTAGON		SLCRBR-IB-1 (P KASTE)	1
WASHINGTON DC 20301		V BOYLE	1
		O BLAKE	1
ATTN LIBRARY	1	R FREY	1
DIRECTOR		G MELANI	1
DEFENSE RESEARCH AND		M CHAWLA	1
ENGINEERING		R FREY	1
WASHINGTON DC 20305		J TRIMBLE	1
		TECHNICAL LIBRARY	1
ATTN LIBRARY	1	ARMY RESEARCH LABORATORY	
DIRECTOR		ABERDEEN PROVING GROUND	
DEFENSE ADVANCED RESEARCH		ABERDEEN MD 21005-5066	
PROJECTS AGENCY			
1400 WILSON BLVD		ATTN LIBRARY	1
ARLINGTON VA 22209		COMMANDER OFFICER	
		HARRY DIAMOND LABORATORY	
ATTN TECHNICAL LIBRARY	1	2800 POWDER MILL ROAD	
INSTITUTE FOR DEFENSE ANALYSES		ADELPHI MD 20783	
1801 N BEAUREGARD STREET			
ALEXANDRIA VA 22311		ATTN HSHB-EA-A	1
		ARMY ENVIRONMENTAL HYGIENE	
ATTN LIBRARY	1	AGENCY	
COMMANDING GENERAL		ABERDEEN PROVING GROUND	
MARINE CORPS DEVELOPMENT AND		ABERDEEN MD 21005	
EDUCATION COMMAND			
MARINE CORPS LANDING FORCE		ATTN J BARKELEY	1
DEVELOPMENT CENTER		ARMY MEDICAL BIOENGINEERING	
QUANTICO VA 22134		RESEARCH AND DEVELOPMENT	
		LABORATORY	
ATTN DRSAR-IRC	1	FORT DIETRICK MD 21701	
DRSAR-LEM (R FREEMAN)	1		
DRSAR-SF (R YOUNG)	1	ATTN G R HUSK	1
ARMY ARMAMENT MUNITIONS AND		COMMANDER	
CHEMICAL COMMAND		ARMY RESEARCH OFFICE	
ROCK ISLAND IL 61299-6000		P. O. BOX 12211	
		RESEARCH TRIANGLE PARK	
ATTN TECHNICAL LIBRARY	1	NC 27709-2211	
ARMY ARMAMENT RESEARCH AND			
DEVELOPMENT COMMAND		ATTN DRXTH-TE-D	1
DOVER NJ 07801		ARMY TOXIC AND HAZARDOUS	
		MATERIALS AGENCY	
		ABERDEEN PROVING GROUND	
		ABERDEEN MD 21005	

DISTRIBUTION (Cont.)

	<u>Copies</u>		<u>Copies</u>
ATTN SMCCR-DDP COMMANDER ARMY CHEMICAL RESEARCH DEVELOPMENT AND ENGINEERING CENTER ABERDEEN PROVING GROUND MD 21010-5423	1	ATTN TECHNICAL LIBRARY SANDIA NATIONAL LABORATORIES P. O. BOX 969 LIVERMORE CA 94550-0096	1
ATTN WL/MNME WL/MNMW WL/MNOI WL/MNME (G GLENN) WL/MNMF (R MABREY) WL/MNME (R MCKINNEY) WL/MNMW (J FOSTER) AIR FORCE ARMAMENT DIVISION EGLIN AIR FORCE BASE FL 32542-6009	1 1 1 1 1 1 1	ATTN STRUCTURAL AND SHOCK CHEMISTRY DIVISION 1153 (MARK U ANDERSON) SANDIA NATIONAL LABORATORIES ALBUQUERQUE NM 87185-5800	1
ATTN T MATUSKO AIR FORCE OFFICE OF SCIENTIFIC RESEARCH BOLLING AIR FORCE BASE WASHINGTON DC 20332	1	ATTN RECORDS CONTROL FOR RICHARD ANDERSON TECHNICAL LIBRARY ARGONNE NATIONAL LABORATORY 9700 SOUTH CASS AVENUE ARGONNE IL 60439	1 1
ATTN TECHNICAL LIBRARY M FINGER C M TARVER E LEE P URTIEW J D HALLQUIST L M ERICKSON E JAMES UNIVERSITY OF CALIFORNIA LAWRENCE LIVERMORE NATIONAL LABORATORY P. O. BOX 808 LIVERMORE CA 94550	1 1 1 1 1 1 1 1	ATTN T W CHRISTIAN THE JOHNS HOPKINS UNIVERSITY APPLIED PHYSICS LABORATORY CHEMICAL PROPULSION INFORMATION AGENCY JOHNS HOPKINS ROAD LAUREL MD 20707	1
ATTN J. REPA M. J. URIZAR S. W. PETERSON L. SMITH C. FOREST C. MORRIS A. W. CAMPBELL R. ENGELKE P. C. CRAWFORD LOS ALAMOS NATIONAL LABORATORY LOS ALAMOS NM 87545	1 1 1 1 1 1 1 1 1	ATTN TECHNICAL LIBRARY THE JOHNS HOPKINS UNIVERSITY APPLIED PHYSICS LABORATORY JOHNS HOPKINS ROAD LAUREL MD 20707	1
		ATTN CODE TERA (J JOYNER) TECHNICAL LIBRARY NEW MEXICO INSTITUTE OF MINING TECHNOLOGY SOCORRO NM 87801	1 1
		ATTN LIBRARY E LIZKA APPLIED RESEARCH LABORATORY PENNSYLVANIA STATE UNIVERSITY P. O. BOX 30 UNIVERSITY PARK STATE COLLEGE PA 16801	1 1

DISTRIBUTION (Cont.)

	<u>Copies</u>		<u>Copies</u>
DEFENSE TECHNICAL INFORMATION CENTER		ATTN M CHICK	1
CAMERON STATION		D D RICHARDSON	1
ALEXANDRIA VA 22304-6142	12	D A JONES	1
		M PODLESAK	1
ATTN LIBRARY	1	MATERIALS RESEARCH LABORATORY	
B HAMMANT	1	P O BOX 50	
P HART	1	ASCOT VALE VICTORIA 3032	
P HASKINS	1	AUSTRALIA	
ROYAL ARMAMENT RESEARCH AND DEVELOPMENT ESTABLISHMENT		ATTN S JACOBS	1
FORTHALSTEAD SEVENOAKS KENT		W PICKLER	1
UNITED KINGDOM		T P LIDDIARD	1
		J W WATT	1
ATTN LIBRARY	1	ADVANCED TECHNOLOGY AND RESEARCH INC	
H R JAMES	1	LAUREL TECHNOLOGY CENTER	
ATOMIC WEAPONS ESTABLISHMENT		14900 SWEITZER LANE	
FOULNESS ISLAND		LAUREL MD 20707	
ESSEX SS3 9XE			
UNITED KINGDOM		ATTN R CHURCH	1
		TRW	
ATTN LIBRARY	1	SAN BERNADINO CA 92401	
P LEE	1		
R H MARTIN	1	ATTN G CHIN	1
ROYAL ORDNANCE PLC		AEROJET ORDNANCE AND MANUFACTURING COMPANY	
WESTCOTT AYLESBURY		9236 EAST HALL ROAD	
BUCKINGHAMSHIRE		DOWNEY CA 90241	
HP18 ONZ			
UNITED KINGDOM		ATTN A MELLOR	1
ATTN DAVID KENNEDY	1	VANDERBILT UNIVERSITY	
ICI EXPLOSIVES GROUP		NASHVILLE TN 37235	
ICI AUSTRALIA OPERATIONS			
PARTY LTD		ATTN R HODGES	1
GATE 1 BALLARAT ROAD		J SMITH	1
DEER PARK		LOCKHEED MISSILES AND SPACE COMPANY	
VICTORIA 3023		P O BOX 504	
AUSTRALIA		SUNNYVALE CA 94086	
ATTN P JONES	1	ATTN G WILLIAMS	1
THE BRITISH EMBASSY		HERCULES INCORPORATED	
BRITISH DEFENCE STAFF		ROCKET CENTER	
3100 MASSACHUSETTS AVENUE NW		P O BOX 210	
WASHINGTON DC 20008		ROCKET CENTER WV 26726	

DISTRIBUTION (Cont.)

	<u>Copies</u>		<u>Copies</u>
ATTN M KLAKKEN	1	INTERNAL DISTRIBUTION (Cont)	
M BERGER	1	R10	1
L LOSEE	1	R101	1
T SPEED	1	R10 (R BERNECKER)	1
HERCULES		R10A (L DICKINSON)	1
BACCHUS WORKS		R10A1	1
MAGNA UT 84044-0098		R10A2	1
ATTN D JEFF JONES		R10B (H S HAISS)	1
MATERIALS AND		R11	1
PROCESS DEVELOPMENT	1	R12	1
THIOKOL CORPORATION		R12 (B A BAUDLER)	1
TACTICAL OPERATIONS		(B GLANCY)	1
HUNTSVILLE DIVISION		(L C HUDSON)	1
P. O. BOX 400006		(G LAIB)	1
HUNTSVILLE AL 35815-1506		(L L MENSI)	1
		(L J MONTESI)	1
ATTN LARRY LEE	1	(P F SPAHN)	1
KTECH CORPORATION		(T SPIVAK)	1
901 PENNSYLVANIA AVENUE			
ALBUQUERQUE NM 87110		R13	1
		R13 (K D ASHWELL)	1
ATTN K L CHRISTIANSON		(R N BAKER)	5
J L HOULTON	1	(R D BARDO)	1
G JOHNSON	1	(A BROWN)	1
ALLIANT TECHSYSTEMS INC		(C S COFFEY)	1
7225 NORTHLAND DRIVE		(J DAVIS)	1
BROOKLYN PARK MN 55428		(D L DEMSKE)	1
		(J W FORBES)	1
ATTN GIFT AND EXCHANGE		(R H GUIRGUIS)	1
DIVISION	1	(P K GUSTAVSON)	1
LIBRARY OF CONGRESS		(R N HAY)	1
WASHINGTON DC 20540		(H D JONES)	1
		(K KIM)	1
ATTN J MORDIN	1	(R J LEE)	1
SCANDOC		(W W LEE)	1
5827 COLUMBIA PIKE		(E R LEMAR)	1
SUITE 501		(P J MILLER)	1
FALLS CHURCH VA 22041		(C T RICHMOND)	1
		(H W SANDUSKY)	1
INTERNAL DISTRIBUTION		(G T SUTHERLAND)	1
E231	2	(D G TASKER)	5
E232	3	(W H WILSON)	1
E342	1	(D L WOODY)	1
G13 (D L DICKINSON)	1	(F J ZERILLI)	1
G13 (T WASMOND)	1	R14	1
G22 (W H HOLT)	1	R14 (J W KOENIG)	1
(W MOCK)	1	R15	1
(S S WAGGENER)	1	R15 (S COLLIGNON)	1

NSWCDD/TR-92/218

DISTRIBUTION (Cont.)

	<u>Copies</u>		<u>Copies</u>
INTERNAL DISTRIBUTION (Cont)			
R42 (R DEWITT)	1	U12 (C SMITH)	1
U10 (W WASSMANN)	1	(W HINCKLEY)	1
U11 (R PLENCE)	1	U32 (G PARRENT)	1
(D HINELY)	1	U43 (L LIPTON)	1

REPORT DOCUMENTATION PAGE

Form Approved
OMB No. 0704-0188

Public reporting burden for this collection of information is estimated to average 1 hour per response, including the time for reviewing instructions, searching existing data sources, gathering and maintaining the data needed, and completing and reviewing the collection of information. Send comments regarding this burden estimate or any other aspect of this collection of information, including suggestions for reducing this burden, to Washington Headquarters Services, Directorate for Information Operations and Reports, 1215 Jefferson Davis Highway, Suite 1204, Arlington, VA 22202-4302, and to the Office of Management and Budget, Paperwork Reduction Project (0704-0188), Washington, DC 20503.

1. AGENCY USE ONLY (Leave blank)		2. REPORT DATE March 1993		3. REPORT TYPE AND DATES COVERED	
4. TITLE AND SUBTITLE The Measurement of Electrical Conductivity in Detonating Condensed Explosives				5. FUNDING NUMBERS	
6. AUTHOR(S) Douglas G. Tasker, Richard J. Lee, and Paul K. Gustavson					
7. PERFORMING ORGANIZATION NAME(S) AND ADDRESS(ES) Naval Surface Warfare Center Dahlgren Division White Oak Detachment 10901 New Hampshire Avenue Silver Spring, MD 20903-5000				8. PERFORMING ORGANIZATION REPORT NUMBER NSWCDD/TR-92/218	
9. SPONSORING/MONITORING AGENCY NAME(S) AND ADDRESS(ES) Office of Chief of Naval Research Dr. R. A. Roberts 800 N. Quincy Street, BCT 1 Arlington, VA 22217-5000				10. SPONSORING/MONITORING AGENCY REPORT NUMBER	
11. SUPPLEMENTARY NOTES					
12a. DISTRIBUTION/AVAILABILITY STATEMENT Approved for public release; distribution is unlimited.				12b. DISTRIBUTION CODE	
13. ABSTRACT (Maximum 200 words) The time-resolved measurement of electrical conductivity provides a unique means of studying detonating explosives. The results of a large number of experiments are reported. Two types of experiments were performed; they measured bulk resistance and time-resolved conductivity. Some interesting effects, due to detonation wave instabilities, were observed when the explosives' dimensions were close to criticality, i.e., close to failure diameter or thickness. The conductivity profile observed in the aluminized explosive PBXN-111 (formerly PBXW-115) is interesting and unusual. The results are probably due to a combination of wave instabilities and late reaction effects. This demonstrates one of the advantages of using conductivity measurements as a diagnostic tool. Wave instabilities are apparent that could not be determined by other means.					
14. SUBJECT TERMS Explosives Detonation wave PBX-9501 PBXW-113 Aluminized explosives instabilities PBX-9502 PBXW-115 Electrical conductivity PBX-9404 PBXW-108 PBXN-111				15. NUMBER OF PAGES 61	
				16. PRICE CODE	
17. SECURITY CLASSIFICATION OF REPORT UNCLASSIFIED	18. SECURITY CLASSIFICATION OF THIS PAGE UNCLASSIFIED	19. SECURITY CLASSIFICATION OF ABSTRACT UNCLASSIFIED	20. LIMITATION OF ABSTRACT SAR		

GENERAL INSTRUCTIONS FOR COMPLETING SF 298

The Report Documentation Page (RDP) is used in announcing and cataloging reports. It is important that this information be consistent with the rest of the report, particularly the cover and its title page. Instructions for filling in each block of the form follow. It is important to *stay within the lines* to meet optical scanning requirements.

Block 1. Agency Use Only (Leave blank).

Block 2. Report Date. Full publication date including day, month, and year, if available (e.g. 1 Jan 88). Must cite at least the year.

Block 3. Type of Report and Dates Covered. State whether report is interim, final, etc. If applicable, enter inclusive report dates (e.g. 10 Jun 87 - 30 Jun 88).

Block 4. Title and Subtitle. A title is taken from the part of the report that provides the most meaningful and complete information. When a report is prepared in more than one volume, repeat the primary title, add volume number, and include subtitle for the specific volume. On classified documents enter the title classification in parentheses.

Block 5. Funding Numbers. To include contract and grant numbers; may include program element number(s), project number(s), task number(s), and work unit number(s). Use the following labels:

C - Contract	PR - Project
G - Grant	TA - Task
PE - Program Element	WU - Work Unit Accession No.

BLOCK 6. Author(s). Name(s) of person(s) responsible for writing the report, performing the research, or credited with the content of the report. If editor or compiler, this should follow the name(s).

Block 7. Performing Organization Name(s) and Address(es). Self-explanatory.

Block 8. Performing Organization Report Number. Enter the unique alphanumeric report number(s) assigned by the organization performing the report.

Block 9. Sponsoring/Monitoring Agency Name(s) and Address(es). Self-explanatory.

Block 10. Sponsoring/Monitoring Agency Report Number. (If Known)

Block 11. Supplementary Notes. Enter information not included elsewhere such as: Prepared in cooperation with...; Trans. of...; To be published in... . When a report is revised, include a statement whether the new report supersedes or supplements the older report.

Block 12a. Distribution/Availability Statement. Denotes public availability or limitations. Cite any availability to the public. Enter additional limitations or special markings in all capitals (e.g. NOFORN, REL, ITAR).

DOD - See DoDD S230.24, "Distribution Statements on Technical Documents."
DOE - See authorities.
NASA - See Handbook NHB 2200.2
NTIS - Leave blank.

Block 12b. Distribution Code.

DOD - Leave blank.
DOE - Enter DOE distribution categories from the Standard Distribution for Unclassified Scientific and Technical Reports.
NASA - Leave blank.
NTIS - Leave blank.

Block 13. Abstract. Include a brief (*Maximum 200 words*) factual summary of the most significant information contained in the report.

Block 14. Subject Terms. Keywords or phrases identifying major subjects in the report.

Block 15. Number of Pages. Enter the total number of pages.

Block 16. Price Code. Enter appropriate price code (*NTIS only*)

Blocks 17.-19. Security Classifications. Self-explanatory. Enter U.S. Security Classification in accordance with U.S. Security Regulations (i.e., UNCLASSIFIED). If form contains classified information, stamp classification on the top and bottom of the page.

Block 20. Limitation of Abstract. This block must be completed to assign a limitation to the abstract. Enter either UL (unlimited) or SAR (same as report). An entry in this block is necessary if the abstract is to be limited. If blank, the abstract is assumed to be unlimited.